

Research Article

Received: 1 July 2013

Revised: 28 August 2013

Accepted: 2 September 2013

Published online in Wiley Online Library

(wileyonlinelibrary.com) DOI: 10.1002/mrc.4014

Computational NMR coupling constants: Shifting and scaling factors for evaluating $^1J_{CH}$

J. San Fabián,^{a*} J. M. García de la Vega,^a R. Suardiáz,^b
M. Fernández-Oliva,^c C. Pérez,^c R. Crespo-Otero^d and R. H. Contreras^e

Optimized shifting and/or scaling factors for calculating one-bond carbon–hydrogen spin–spin coupling constants have been determined for 35 combinations of representative functionals (PBE, B3LYP, B3P86, B97-2 and M06-L) and basis sets (TZVP, HILL-su3, EPR-III, aug-cc-pVTZ-J, ccJ-pVDZ, ccJ-pVTZ, ccJ-pVQZ, pcJ-2 and pcJ-3) using 68 organic molecular systems with 88 $^1J_{CH}$ couplings including different types of hybridized carbon atoms. Density functional theory assessment for the determination of $^1J_{CH}$ coupling constants is examined, comparing the computed and experimental values. The use of shifting constants for obtaining the calculated coupling improves substantially the results, and most models become qualitatively similar. Thus, for the whole set of couplings and for all approaches excluding those using the M06 functional, the root-mean-square deviations lie between 4.7 and 16.4 Hz and are reduced to 4–6.5 Hz when shifting constants are considered. Alternatively, when a specific rovibrational contribution of 5 Hz is subtracted from the experimental values, good results are obtained with PBE, B3P86 and B97-2 functionals in combination with HILL-su3, aug-cc-pVTZ-J and pcJ-2 basis sets. Copyright © 2013 John Wiley & Sons, Ltd.

Supporting information may be found in the online version of this article.

Keywords: density functional; NMR spectroscopy; coupling constants; basis sets

Introduction

During the last years, density functional theory (DFT) has been applied successfully to the prediction of NMR spin–spin coupling constants (SSCCs).^[1–5] However, the DFT bibliographic data related to the calculation of these constants show certain dispersion regarding the functional and basis sets employed.^[1–4,6–14] There are several works reporting that B3LYP^[15,16] functional yields satisfactory results for SSCC in a small set of molecules.^[6–8] Maximoff *et al.*^[9] reported the assessment of 20 different functionals using aug-cc-pVTZ-J basis set for predicting one-bond carbon–hydrogen ($^1J_{CH}$) spin–spin coupling (SSCC). In that work, the best results were reported for PBE,^[17,18] whereas B3LYP^[15,16] was one of the worst. In a similar study, Keal *et al.*^[10] proposed B97-2,^[19,20] functionals to be an acceptable choice for predicting one-bond coupling. More recently, Cunha Neto *et al.*^[14] have analyzed the performance of nine functionals for the calculation of $^1J_{CH}$ in electron-rich systems. They concluded that B3LYP^[15,16] shows the best performance for non-rich electron systems while PBE yields better results for rich electron systems.

It is also known that the basis set determines the quality of the predicted SSCCs. A study of Peralta *et al.*^[12] employing the B3LYP^[15,16] functional and different basis sets suggests the B3LYP/aug-cc-pVTZ-J combination as a good choice in the prediction of X–H (X = N, O, F, H) coupling constants. In our previous work,^[13] a good performance in the prediction of $^1J_{CC}$ coupling constants was found with the B3LYP functional and the economical TZVP^[21,22] basis set.

Recently, Helgaker *et al.*^[1,23] obtained better results when the SSCCs are evaluated at the geometry optimized using the same functional. The SSCCs calculated with geometries optimized with the same functional seem to move the system away from the

triplet instabilities, and thereby, the results become improved. A recent study in norbornane derivatives shows an important effect of the geometry in the calculation of the $^1J_{CH}$ SSCCs.^[24] The authors recommended the B3LYP/aug-cc-pVDZ for geometry optimization and B3LYP/EPR-III for the calculation of the SSCCs. Basis sets effects on the SSCCs have been clearly established, and the importance of s-tight and polarization functions for Fermi contact and non-contact contributions, respectively, is well known. However, the systematic improvement of functionals for these properties is not clear. This is due, in part, to the inability to find the exact exchange–correlation functional. In addition, DFT-calculated SSCC values do not seem to correlate with the quality of the approximation used in the exchange–correlation functional. An alternative to improve the results even with inexpensive functional/basis set is the use of shifting and scaling

* Correspondence to: J. San Fabián, Departamento de Química Física Aplicada, Facultad de Ciencias, Universidad Autónoma de Madrid, 28049 Madrid, Spain. E-mail: jesus.sanfabian@uam.es

^a Departamento de Química Física Aplicada, Facultad de Ciencias, Universidad Autónoma de Madrid, 28049 Madrid, Spain

^b Department de Química and Institut de Biotecnologia i de Biomedicina (IBB), Universitat Autònoma de Barcelona, 08193 Bellaterra, Barcelona, Spain

^c Departamento de Química Física, Facultad de Química, Universidad de La Habana, La Habana 10400, Cuba

^d Max-Planck-Institut für Kohlenforschung, Kaiser-Wilhelm-Platz 1, 45470 Mülheim an der Ruhr, Germany

^e Departamento de Física, Facultad de Ciencias Exactas y Naturales, Universidad de Buenos Aires and IFIBA-CONICET, Buenos Aires, Argentina

factors. Recent reports have appeared in the literature on the development of SSCC-scaled factors.^[13,25] In the present work, we optimize general shifting and/or scaling factors that can be used to obtain $^1J_{CH}$. These optimized factors are derived by correlating computed $^1J_{CH}$, which are obtained by applying 36 functional/basis set combinations over 68 organic molecules containing first and second row elements, with the corresponding experimental values.

Computational Details

There is a large number of reported density functionals in the literature. These are now available for the calculation of SSCC and implemented in many codes.^[1,2] Among this large number, we have selected five exchange–correlation functionals, based on their successful presence in the literature concerning SSCC calculations. The generalized gradient approximated (GGA) functional PBE^[17,18] was selected because of its noteworthy performance for the prediction of $^1J_{CH}$ among other 20 functionals as reported by Maximoff *et al.*^[9] Also, Cunha Neto *et al.*^[14] obtained reliable results using PBE^[17,18] for calculating $^1J_{CH}$ in 2-substituted tetrahydropyrans. M06-L is a meta-generalized functional (meta-GGA)^[26,27] tested to reproduce appropriately some magnetic properties like chemical shifts^[28] and Heisenberg magnetic coupling constants^[29] improving predictions over other functionals. B3P86^[15,30] was the hybrid functional that performed best in Maximoff *et al.* study.^[9] B3LYP^[15,16] has been used with good results by many authors,^[6–8,31,32] although it has been reported as one of the worst by Maximoff *et al.*^[9] Hybrid B97-2^[19] has been suggested by Keal *et al.*^[10] for the calculation of $^1J_{CH}$ in combination with aug-cc-pVTZ-J^[33] basis set. The $^1J_{CH}$ values calculated by Keal *et al.*^[10] using B97-2 functional present mean absolute errors (MAEs) that are similar to those obtained by PBE functional. However, B97-2 results present smaller maximum errors, implying to be the most accurate for the considered couplings.

Computations were performed using nine basis sets of contracted Gaussian functions, namely TZVP,^[21,22] EPR-III,^[34,35] HIII-su3,^[36] aug-cc-pVTZ-J,^[33] ccJ-pVDZ, ccJ-pVTZ, ccJ-pVQZ,^[37] pcJ-2 and pcJ-3.^[38] TZVP^[21,22] is a DFT-optimized valence triple- ζ basis set with promising results for the prediction of hyperfine couplings^[39] and SSCCs^[40–42] in combination with the B3LYP functional. EPR-III^[34,35] is larger and has been optimized for the computation of hyperfine coupling constants by DFT methods with the s-part improved to describe better the nuclear regions; it is a triple- ζ basis including diffuse functions, doubled polarizations and a single set of f-polarization functions. HIII-su3^[36] is the Huzinaga III basis set^[43] in which the s original basis has been uncontracted and augmented with three tight functions. This basis set has been used satisfactorily in the computation of SSCCs.^[10,44–48] aug-cc-pVTZ-J^[33] is a relatively large basis set, specially designed for the computation of SSCCs. aug-cc-pVTZ-J is a recontraction of aug-cc-pVTZ-Juc,^[33] which itself is the triple- ζ aug-cc-pVTZ^[49–52] of Dunning completely uncontracted and augmented with four tight s-type functions and without the most diffuse second polarization function. ccJ-pVXZ^[37] (X = D, T and Q) are hierarchical basis sets based on those of Dunning cc-pVXZ and especially optimized for coupled-cluster calculations of indirect SSCCs. pcJ-X^[38] (X = D and T) are polarization-consistent basis sets optimized for calculations of indirect spin–spin with density functional methods. These two groups of basis sets should offer a systematic convergence as the size of basis set increases. The largest basis sets of these series (ccJ-pV5Z and pcJ-4) are

Table 1. Approximate relative time^a for the calculation of $^1J_{CH}$ in $C_6H_5NO_2$

	PBE	B3LYP	B3P86	B97-2	M06-L
TZVP	1	2	2	2	16
HIII-su3	6	21	20	19	47
EPR-III	8	23	22	25	110
aug-cc-pVTZ-J	14	61	58	59	190
ccJ-pVTZ	10	30	29	25	69
pcJ-2	12	49	50	47	109
ccJ-pVDZ	—	3	—	—	—
ccJ-pVQZ	—	263	—	—	—
pcJ-3	—	548	—	—	—

^aRelative to the time required when using PBE/TZVP.

prohibitive in this study owing to the number and the size of calculated molecules.

The computational cost of the calculations depends on the complexity of the approximate functional expressions and on the basis set dimensions. Relative calculation times for $C_6H_5NO_2$ molecule are shown in Table 1. These values have approximate character because they are partially computer dependent.

In this study, we have considered a collection of 68 organic molecules containing first and second row elements extracted from that used by Maximoff *et al.*^[9] The molecules and the sets of experimental and calculated $^1J_{CH}$ coupling constants are presented in the Supporting Information.

Thirty-three sets of calculations were performed using the fully optimized PBE0/6-31+G(2df,p) geometries. Those sets correspond to $^1J_{CH}$ SSCC calculated with all possible combinations of five functionals (PBE, B3LYP, B3P86, B97-2 and M06-L) and six basis sets (TZVP, HIII-su3, EPR-III, aug-cc-pVTZ-J, ccJ-pVTZ and pcJ-2). Three other calculations were carried out with the B3LYP functional and three basis sets (ccJ-pVDZ, ccJ-pVQZ and pcJ-3) to study the basis set convergence. Two additional sets have been calculated using the same functional/basis set approach for the geometry optimization and for the SSCC calculation. The approaches used for these sets are B3LYP/TZVP and B3P86/aug-cc-pVTZ-J. These two combinations were chosen because they yield the best results for the whole set of couplings with PBE0/6-31+G(2df,p) geometries. These last results will be denoted by a simplified notation with 'g' at the end of the functional/basis set combination (B3LYP/TZVPg and B3P86/aug-cc-pVTZ-Jg) instead of the usual functional/basis-set//functional/basis-set notation.

Although PBE0/6-31+G(2df,p) geometries should be the same as those used by Maximoff *et al.*,^[9] we took a different conformation for some molecules. We use the calculated energy as criterion of conformer selection. For instance, for acrolein ($CH_2 = CH(CHO)$), we took the planar anti-conformer, which is between 2 and 2.3 kcal/mol and is more stable than the syn conformer when optimized at PBE0/6-31+G(2df,p), B3LYP/TZVP or B3P86/aug-cc-pVTZ-J levels.

Evaluation of solvent effect in small molecules has shown reduced sensitivity. This effect is mainly due to reaction field effects via the indirect contribution from equilibrium geometry changes.^[53,54] Hence, solvent effects are neglected. $^1J_{CH}$ values in non-rigid molecules that contain chemical groups with free rotation (e.g. methyl) have been averaged over equivalent pairs of atoms. All computations were performed using the Gaussian03 revision E1^[55] and Gaussian09 revision A2.^[56]

Q2

T1

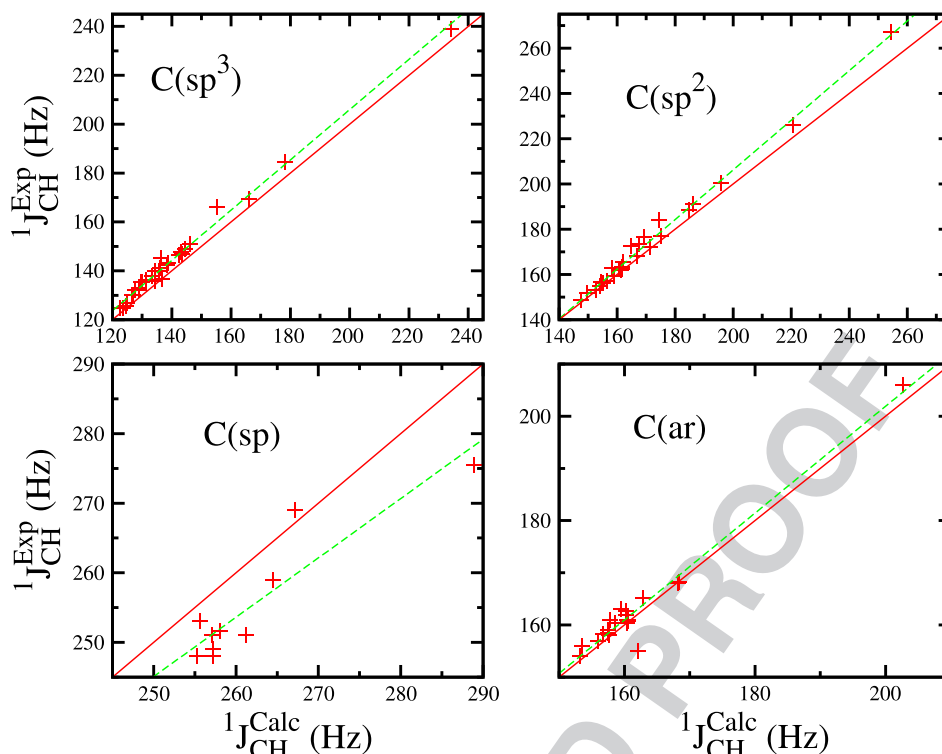


Figure 1. Calculated against experimental $^1J_{CH}$ couplings for sets involving sp^3 , sp^2 , sp and ar carbon. DFT constants have been carried out using B3LYP/TZVPg. Dashed lines represent the least-squared fit to Eqn (1).

Results and Discussion

The statistical analysis of the 88 $^1J_{CH}$ coupling constants has been carried out over five sets of data: set-1 includes the whole data set of couplings (88 values), set-2 includes those couplings that involve sp^3 hybridized carbon atoms (30 values), set-3 is formed by those couplings with sp^2 hybridized carbon atoms (27 values), set-4 contains couplings involving sp hybridized carbon atoms (10 values), and set-5 includes coupling values that involve aromatic carbon atoms (21 values).

Besides the aforementioned sets, the calculated $^1J_{CH}$ values were shifted and/or scaled to obtain better estimations and to detect whether the differences between the results are merely either quantitative or qualitative. Those fitted values could allow for systematic deviations in the calculated couplings owing to either the rovibrational contributions or the computational level used to optimize the geometries or to calculate the coupling constants. The representation of experimental against calculated SSCCs for the four type of couplings (Fig. 1) shows a linear dependence (dashed lines). Four groups of calculated/fitted couplings are considered. These groups are obtained using the following linear correction between calculated and experimental $^1J_{CH}$ values,

$$^1J_{CH}^{Exp} = a^{(i)} + b^{(i)} \cdot ^1J_{CH}^{Calc} \quad (1)$$

First group ($i = 0$ in Eqn (1)) corresponds to the original calculated values, that is, $a^{(0)} = 0$ and $b^{(0)} = 1$. In the second group ($i = 1$), only the independent terms, $a^{(1)}$, are fitted ($b^{(1)} = 1$); that is, the $^1J_{CH}$ values are recalculated using a shifting constant for each functional/basis set combination. The third group ($i = 2$) corresponds to that obtained using fitted independent, $a^{(2)}$, and linear, $b^{(2)}$, terms calculated by fitting the $^1J_{CH}$ values for each functional/basis model. Finally, the fourth group (named $i = rv$) is a particular case of second group where the same constant

shift for all models is used to include an estimated rovibrational contribution.

A proper comparison with experimental values should be carried out including the rovibrational contributions in the equilibrium calculated values. The collection of molecules considered in this work is too large to make a deep study of the rovibrational contributions to $^1J_{CH}$. However, a rough estimation for this contribution between 4 and 5.5 Hz could be assumed, at least for most of the molecules, considering the following values from the literature: methane 4.43 Hz,^[57,58] ethylene 5.1 Hz,^[59] acetylene 4.86 Hz^[60] and hydrogen cyanide 5.1 Hz.^[59] These contributions should be added to the equilibrium values to approximate the experimental figures. In the present work, a rovibrational contribution of $a^{(rv)} = 5$ Hz has been considered. Coefficients $a^{(1)}$, $a^{(2)}$ and $b^{(2)}$ were obtained by fitting the calculated SSCCs for each set of couplings and for each approach (functional/basis set combination) to the corresponding Eqn (1). The values of these coefficients are presented in Tables 2–6 and in the Supporting Information. Statistics for the five data sets and for the different groups of calculated and fitted values are based on standard deviation (σ), minimum (min) deviation and maximum (max) deviation,

$$\sigma = \sqrt{\frac{\sum (J_{CH}^{Exp} - J_{CH}^{Calc})^2}{n - 1}} \quad (2)$$

Statistical results ($\sigma^{(i)}$, $\min^{(i)}$ and $\max^{(i)}$) are presented in Tables 2–6 and in the Supporting Information. Additional statistical parameters as MAE and relative MAE do not present qualitative differences, and they were given in the Supporting Information. The numerical data for the linear approach ($i = 2$) have only been shown in the Supporting Information for two reasons: small qualitative differences as regards the displacement approach and the

Table 2. Statistical results (in hertz) for data set-1 (whole data) using the indicated functional/basis set. γ -intercept ($a^{(1)}$) for fits to Eqn (1) and its standard deviation (between parentheses) are given

Func./basis set	Original values			Shifted using Eqn (1)				5 Hz of rovib. contr.		
	$\sigma^{(0)}$	min ⁽⁰⁾	max ⁽⁰⁾	$a^{(1)}$	$\sigma^{(1)}$	min ⁽¹⁾	max ⁽¹⁾	$\sigma^{(rv)}$	min ^(rv)	max ^(rv)
PBE/TZVP	16.4	−36.3	−4.3	15.61 (0.5)	4.7	−20.7	11.3	11.7	−31.3	0.7
PBE/HIII-su3	8.5	−21.3	8.0	6.94 (0.5)	4.8	−14.3	14.9	5.2	−16.3	13.0
PBE/EPR-III	12.0	−27.7	0.7	11.08 (0.5)	4.3	−16.6	11.8	7.5	−22.7	5.7
PBE/aug-cc-pVTZ-J	7.6	−19.9	10.0	5.89 (0.5)	4.8	−14.0	15.9	4.9	−14.9	15.0
PBE/ccJ-pVTZ	9.6	−25.2	5.4	8.37 (0.5)	4.7	−16.9	13.8	5.8	−20.2	10.4
PBE/pcJ-2	6.7	−19.0	11.0	4.73 (0.5)	4.8	−14.3	15.7	4.8	−14.0	16.0
B3LYP/TZVP	5.5	−16.8	14.6	2.07 (0.5)	5.1	−14.7	16.7	5.8	−11.8	19.6
B3LYP/HIII-su3	11.2	−1.2	30.9	−9.12 (0.7)	6.4	−10.3	21.8	15.6	3.8	35.9
B3LYP/EPR-III	7.1	−5.2	22.8	−4.60 (0.6)	5.4	−9.8	18.2	11.1	−0.2	27.8
B3LYP/aug-cc-pVTZ-J	12.1	−0.0	32.6	−10.14 (0.7)	6.5	−10.2	22.5	16.5	5.0	37.6
B3LYP/ccJ-pVDZ	9.1	−6.1	27.2	−6.59 (0.7)	6.2	−12.7	20.6	13.2	−1.1	32.2
B3LYP/ccJ-pVTZ	9.5	−2.5	27.7	−7.32 (0.6)	5.9	−9.8	20.4	13.7	2.5	32.7
B3LYP/ccJ-pVQZ	11.5	−0.7	31.3	−9.51 (0.7)	6.3	−10.2	21.8	15.9	4.3	36.3
B3LYP/pcJ-2	12.4	0.4	32.9	−10.58 (0.7)	6.4	−10.1	22.4	16.9	5.4	37.9
B3LYP/pcJ-3	11.8	−0.4	31.9	−9.80 (0.7)	6.4	−10.2	22.1	16.2	4.6	36.9
B3P86/TZVP	15.6	−34.3	−4.8	14.94 (0.5)	4.3	−19.4	10.1	10.9	−29.3	0.2
B3P86/HIII-su3	6.5	−16.9	9.8	4.62 (0.5)	4.6	−12.3	14.4	4.6	−11.9	14.8
B3P86/EPR-III	9.3	−23.3	2.8	8.35 (0.4)	4.1	−15.0	11.2	5.3	−18.3	7.8
B3P86/aug-cc-pVTZ-J	5.7	−15.5	12.0	3.25 (0.5)	4.6	−12.3	15.2	4.9	−10.5	17.0
B3P86/ccJ-pVTZ	7.4	−20.3	7.3	5.95 (0.5)	4.4	−14.4	13.3	4.5	−15.3	12.3
B3P86/pcJ-2	5.8	−15.9	11.6	3.46 (0.5)	4.6	−12.5	15.1	4.8	−10.9	16.6
B97-2/TZVP	14.0	−32.7	−2.5	13.15 (0.5)	4.5	−19.6	10.7	9.3	−27.7	2.5
B97-2/HIII-su3	7.8	−21.2	5.3	6.40 (0.5)	4.3	−14.8	11.7	4.5	−16.2	10.3
B97-2/EPR-III	11.4	−28.1	−2.1	10.60 (0.4)	4.0	−17.5	8.5	6.9	−23.1	2.9
B97-2/aug-cc-pVTZ-J	6.2	−18.9	8.8	4.17 (0.5)	4.5	−14.7	13.0	4.6	−13.9	13.8
B97-2/ccJ-pVTZ	9.5	−26.1	1.7	8.45 (0.5)	4.3	−17.6	10.1	5.5	−21.1	6.7
B97-2/pcJ-2	7.3	−20.4	6.9	5.76 (0.5)	4.4	−14.7	12.7	4.5	−15.4	11.9
M06-L/TZVP	44.8	24.5	86.2	−42.17 (1.5)	14.5	−17.7	44.1	49.6	29.5	91.2
M06-L/HIII-su3	42.8	22.8	85.1	−39.89 (1.6)	14.9	−17.1	45.3	47.5	27.8	90.1
M06-L/EPR-III	43.6	24.4	84.2	−41.19 (1.5)	13.7	−16.8	43.0	48.4	29.4	89.2
M06-L/aug-cc-pVTZ-J	38.2	20.1	79.3	−35.48 (1.5)	13.7	−15.4	43.8	43.0	25.1	84.3
M06-L/ccJ-pVTZ	43.3	24.9	83.1	−40.85 (1.4)	13.6	−16.0	42.3	48.1	29.9	88.1
M06-L/pcJ-2	46.3	28.4	83.7	−44.37 (1.3)	12.4	−15.9	39.3	51.2	33.4	88.7
B3LYP/TZVPg	4.7	−12.7	13.4	1.94 (0.5)	4.3	−10.8	15.3	5.3	−7.7	18.4
B3P86/aug-cc-pVTZ-Jg	5.9	−14.7	9.9	4.12 (0.4)	4.2	−10.6	14.0	4.3	−9.7	14.9

existence of a strong correlation between independent and linear terms for this kind of SSCCs.

The whole data set (set-1) covers an experimental range between 125 and 275 Hz. For this set, the best results are those of the inexpensive B3LYP/TZVPg and B3LYP/TZVP with $\sigma^{(0)}$ of 4.7 and 5.5 Hz, respectively. Other results with $\sigma^{(0)}$ values close to those are B3P86/aug-cc-pVTZ-J, B3P86/pcJ-2, B3P86/aug-cc-pVTZ-Jg, B97-2/aug-cc-pVTZ-J, B3P86/HIII-su3 and PBE/pcJ-2 with $\sigma^{(0)}$ smaller than 7 Hz. The worst results are those obtained for M06-L functional with any basis set ($\sigma^{(0)}$ between 38 and 46 Hz) and those obtained with PBE, B3P86 and B97-2 functionals and the TZVP basis set with $\sigma^{(0)}$ of 16.4, 15.6 and 14.0 Hz, respectively.

Considering B3LYP/TZVPg results, only four calculated values deviate more than 10 Hz in magnitude from the experimental ones. These correspond to the following molecules: $\text{CH}_2\text{F}(\text{CN})$ (sp^3 -carbon, deviation of −11 Hz), $\text{CH}(\text{O})\text{F}$ (sp^2 , −13 Hz), $\text{HCC}(\text{CH}_2\text{CN})$ (sp , 10 Hz) and HCCF (sp , 13 Hz).

Significant improvement is obtained for all the results when fitted intercepts ($a^{(1)}$ in Eqn (1)) were considered. The resulting $\sigma^{(1)}$ values have an interval between 4.0 Hz (B97-2/EPR-III) and 6.5 Hz (B3LYP/aug-cc-pVTZ-J) excluding those obtained with the M06-L functional whose $\sigma^{(1)}$ deviations range between 12.4 and 14.9 Hz. It is interesting that, excluding the M06-L results, the largest $\sigma^{(1)}$ (between 5.1 and 6.5 Hz) correspond to the B3LYP results. The intercepts $a^{(1)}$ are always negative (between −4.6 and −10.6 Hz) for those results unless TZVP basis set is used (2.1 Hz). Besides the B3LYP results, only the M06-L ones present negative $a^{(1)}$ intercepts. Therefore, the B3LYP and M06-L functionals yield, in general, coupling constants larger than the experimental (excepting the B3LYP/TZVP) while the remaining functionals yield values smaller than the experimental (see Fig. 2 and Supporting Information).

When a constant factor a^{rv} of 5 Hz is considered, several models (functional/basis set) give $\sigma^{(rv)}$ deviations smaller than 5 Hz. These are PBE, B3P86 and B97-2 with aug-cc-pVTZ-J and pcJ-2,

Table 3. Statistical results (in hertz) for data set-2 (sp^3 hybridized carbon atoms) using the indicated functional/basis set. γ -intercept ($\sigma^{(1)}$) for fits to Eqn (1) and its standard deviation (between parentheses) are given

Func./basis set	Original values			Shifted using Eqn (1)				5 Hz of rovib. contr.		
	$\sigma^{(0)}$	min ⁽⁰⁾	max ⁽⁰⁾	$\sigma^{(1)}$	$\sigma^{(1)}$	min ⁽¹⁾	max ⁽¹⁾	$\sigma^{(rv)}$	min ^(rv)	max ^(rv)
PBE/TZVP	17.5	-25.3	-11.7	16.92 (0.6)	3.4	-8.3	5.2	12.6	-20.3	-6.7
PBE/HIII-su3	9.5	-16.9	-4.2	8.88 (0.5)	2.9	-8.0	4.7	4.9	-11.9	0.8
PBE/EPR-III	12.8	-20.4	-7.3	12.26 (0.6)	3.1	-8.2	4.9	8.0	-15.4	-2.3
PBE/aug-cc-pVTZ-J	8.5	-15.6	-3.4	7.95 (0.5)	2.7	-7.6	4.6	4.0	-10.6	1.6
PBE/ccJ-pVTZ	10.4	-17.7	-4.9	9.79 (0.6)	3.0	-7.9	4.9	5.7	-12.7	0.1
PBE/pcJ-2	7.4	-14.4	-2.2	6.78 (0.5)	2.7	-7.6	4.6	3.2	-9.4	2.8
B3LYP/TZVP	5.6	-11.8	-0.9	4.98 (0.4)	2.5	-6.9	4.1	2.5	-6.8	4.1
B3LYP/HIII-su3	5.7	-1.2	9.2	-5.18 (0.4)	2.1	-6.4	4.0	10.6	3.8	14.2
B3LYP/EPR-III	2.7	-5.2	5.7	-1.55 (0.4)	2.2	-6.8	4.2	7.0	-0.2	10.7
B3LYP/aug-cc-pVTZ-J	6.5	-0.0	10.2	-6.11 (0.4)	2.0	-6.2	4.1	11.5	5.0	15.2
B3LYP/ccJ-pVDZ	4.2	-3.7	7.6	-3.20 (0.5)	2.6	-6.9	4.4	8.7	1.3	12.6
B3LYP/ccJ-pVTZ	4.6	-2.5	8.2	-3.95 (0.4)	2.1	-6.4	4.3	9.4	2.5	13.2
B3LYP/ccJ-pVQZ	6.1	-0.7	9.8	-5.65 (0.4)	2.1	-6.3	4.1	11.0	4.3	14.8
B3LYP/pcJ-2	7.0	0.4	10.7	-6.58 (0.4)	2.0	-6.1	4.1	12.0	5.4	15.7
B3LYP/pcJ-3	6.3	-0.4	9.9	-5.84 (0.4)	2.0	-6.2	4.1	11.2	4.6	14.9
B3P86/TZVP	16.9	-24.3	-11.8	16.32 (0.6)	3.1	-8.0	4.5	11.9	-19.3	-6.8
B3P86/HIII-su3	7.4	-14.0	-2.4	6.91 (0.4)	2.4	-7.1	4.5	3.1	-9.0	2.6
B3P86/EPR-III	10.4	-17.3	-5.2	9.86 (0.5)	2.7	-7.4	4.6	5.7	-12.3	-0.2
B3P86/aug-cc-pVTZ-J	6.2	-12.5	-1.1	5.64 (0.4)	2.3	-6.9	4.6	2.4	-7.5	3.9
B3P86/ccJ-pVTZ	8.3	-14.8	-3.1	7.74 (0.5)	2.6	-7.1	4.6	3.8	-9.8	1.9
B3P86/pcJ-2	6.4	-12.7	-1.3	5.82 (0.4)	2.3	-6.9	4.6	2.5	-7.7	3.7
B97-2/TZVP	15.7	-22.6	-10.4	15.21 (0.5)	3.0	-7.4	4.8	10.8	-17.6	-5.4
B97-2/HIII-su3	9.0	-15.8	-3.4	8.44 (0.5)	2.8	-7.3	5.0	4.5	-10.8	1.6
B97-2/EPR-III	12.3	-19.6	-6.6	11.74 (0.6)	3.1	-7.9	5.2	7.5	-14.6	-1.6
B97-2/aug-cc-pVTZ-J	7.1	-13.8	-1.9	6.50 (0.5)	2.6	-7.3	4.6	3.0	-8.8	3.1
B97-2/ccJ-pVTZ	10.5	-17.6	-4.7	9.89 (0.6)	3.1	-7.7	5.2	5.9	-12.6	0.3
B97-2/pcJ-2	8.5	-15.3	-3.2	7.92 (0.5)	2.7	-7.4	4.7	4.0	-10.3	1.8
M06-L/TZVP	32.2	24.5	60.3	-30.94 (1.3)	7.0	-6.5	29.4	37.2	29.5	65.3
M06-L/HIII-su3	30.3	22.8	56.2	-29.01 (1.2)	6.7	-6.2	27.2	35.2	27.8	61.2
M06-L/EPR-III	31.6	24.4	60.2	-30.31 (1.3)	7.1	-5.9	29.9	36.6	29.4	65.2
M06-L/aug-cc-pVTZ-J	26.9	20.1	52.9	-25.63 (1.2)	6.6	-5.6	27.2	31.9	25.1	57.9
M06-L/ccJ-pVTZ	31.9	24.9	61.5	-30.50 (1.3)	7.3	-5.7	31.0	36.8	29.9	66.5
M06-L/pcJ-2	35.4	28.4	59.0	-34.26 (1.1)	6.0	-5.8	24.7	40.4	33.4	64.0
B3LYP/TZVPg	4.8	-10.8	0.0	4.27 (0.4)	2.1	-6.5	4.3	2.3	-5.8	5.0
B3P86/aug-cc-pVTZ-Jg	6.6	-13.1	-1.4	6.11 (0.4)	2.3	-7.0	4.7	2.5	-8.1	3.6

B3P86 and B97-2 with HIII-su3, B3P86/ccJ-pVTZ and B3P86/aug-cc-pVTZ-Jg. This last one yields the best $\sigma^{(rv)}$ of 4.3 Hz. It should be noted that now B3LYP results (unless TZVP basis set is used) yield large $\sigma^{(rv)}$ values between 11 and 17 Hz. Moreover, TZVP basis set with PBE, B3P86 and B97-2 functionals gives large $\sigma^{(rv)}$ between 9 and 12 Hz.

Set-2 includes 30 SSCs involving sp^3 hybridized carbon atoms, and it has an experimental range between 125 and 239 Hz. Best results ($\sigma^{(0)}$ smaller than 6 Hz) are those obtained with B3LYP functional used in combination with EPR-III ($\sigma^{(0)} = 2.7$ Hz), ccJ-pVDZ (4.2 Hz), ccJ-pVTZ (4.6 Hz), TZVP (5.6 Hz) and HIII-su3 (5.7 Hz) basis sets. Moreover, good performance is obtained with B3LYP/TZVPg approach ($\sigma^{(0)} = 4.8$ Hz). The worst results are those obtained with M06-L functional ($\sigma^{(0)}$ between 27 and 35 Hz). For B3LYP/EPR-III results, only three couplings deviate more than 5 Hz in magnitude: $\overline{\text{CH}_2\text{N}(\text{CH}_3)_2}$ (deviation of 5.7 Hz, the coupled carbon is the overlined one), CH_4 (5.2 Hz) and $\text{CH}_2\text{F}(\text{CN})$ (-5.2 Hz). When shifted, all combinations improve significantly the results. $\sigma^{(1)}$ deviations are between 2.0 and 3.4 Hz exclud-

ing the M06-L results whose values are between 6.0 and 7.3 Hz. If the rovibrational correction is considered, five models yield $\sigma^{(rv)}$ values smaller than 3 Hz: B3LYP/TZVPg, B3P86/aug-cc-pVTZ-J, B3LYP/TZVP, B3P86/aug-cc-pVTZ-Jg and B3P86/pcJ-2. The remaining B3LYP results and those carried out with TZVP when is not used in combination with B3LYP functional yield large $\sigma^{(rv)}$ values between 7 and 13 Hz.

Set-3 contains 27 couplings involving sp^2 hybridized carbon atoms and ranges between 149 and 267 Hz. Best results are those of B3LYP/TZVPg ($\sigma^{(0)}$ of 4.6 Hz) followed by those of B3LYP functional with EPR-III and TZVP basis sets ($\sigma^{(0)}$ of 5.1 and 5.3 Hz, respectively). B3P86/aug-cc-pVTZ-J, B3P86/pcJ-2 and B3P86/aug-cc-pVTZ-Jg also give acceptable results ($\sigma^{(0)}$ of 5.5, 5.6 and 5.9 Hz, respectively). Again, the worst results correspond to those of M06-L functional ($\sigma^{(0)}$ between 36 and 42 Hz). Additionally, TZVP, EPR-III and ccJ-pVTZ basis sets yield unsatisfactory results for all functionals ($\sigma^{(0)}$ between 10 and 18 Hz) excepting for B3LYP, as indicated earlier. All calculated values with B3LYP/TZVPg are smaller than the experimental ones. Six values present

Q4

Table 4. Statistical results (in hertz) for data set-3 (sp^2 hybridized carbon atoms) using the indicated functional/basis set. γ -intercept ($\sigma^{(1)}$) for fits to Eqn (1) and its standard deviation (between parentheses) are given

Func./basis set	Original values			Shifted using Eqn (1)				5 Hz of rovib. contr.		
	$\sigma^{(0)}$	min ⁽⁰⁾	max ⁽⁰⁾	$\sigma^{(1)}$	$\sigma^{(1)}$	min ⁽¹⁾	max ⁽¹⁾	$\sigma^{(rv)}$	min ^(rv)	max ^(rv)
PBE/TZVP	18.5	-36.3	-12.8	17.38 (1.0)	5.4	-18.9	4.6	13.7	-31.3	-7.8
PBE/HIII-su3	9.4	-21.3	-4.5	8.31 (0.8)	4.0	-13.0	3.8	5.2	-16.3	0.5
PBE/EPR-III	13.4	-27.7	-8.4	12.36 (0.9)	4.5	-15.3	3.9	8.8	-22.7	-3.4
PBE/aug-cc-pVTZ-J	8.3	-19.9	-3.5	7.16 (0.8)	4.0	-12.7	3.7	4.5	-14.9	1.5
PBE/ccJ-pVTZ	11.0	-25.2	-5.8	9.85 (0.9)	4.6	-15.4	4.0	6.7	-20.2	-0.8
PBE/pcJ-2	7.3	-19.0	-2.5	5.99 (0.8)	4.0	-13.0	3.5	4.1	-14.0	2.5
B3LYP/TZVP	5.3	-16.8	0.5	3.34 (0.8)	4.1	-13.5	3.9	4.4	-11.8	5.5
B3LYP/HIII-su3	9.0	1.1	12.5	-8.34 (0.5)	2.8	-7.2	4.2	13.9	6.1	17.5
B3LYP/EPR-III	5.1	-5.2	7.9	-3.86 (0.6)	3.2	-9.1	4.1	9.6	-0.2	12.9
B3LYP/aug-cc-pVTZ-J	10.0	2.8	13.7	-9.45 (0.5)	2.8	-6.6	4.2	15.0	7.8	18.7
B3LYP/ccJ-pVDZ	6.9	-6.1	9.9	-5.54 (0.8)	4.0	-11.7	4.4	11.5	-1.1	14.9
B3LYP/ccJ-pVTZ	7.3	-2.3	10.5	-6.41 (0.6)	3.2	-8.7	4.1	12.1	2.7	15.5
B3LYP/ccJ-pVQZ	9.4	1.6	12.9	-8.74 (0.6)	3.0	-7.1	4.2	14.3	6.6	17.9
B3LYP/pcJ-2	10.5	3.3	14.2	-9.89 (0.5)	2.8	-6.6	4.3	15.4	8.3	19.2
B3LYP/pcJ-3	9.7	2.4	13.4	-9.10 (0.5)	2.8	-6.7	4.3	14.6	7.4	18.4
B3P86/TZVP	17.5	-34.3	-12.3	16.44 (1.0)	5.0	-17.9	4.1	12.7	-29.3	-7.3
B3P86/HIII-su3	6.7	-16.9	-2.3	5.57 (0.7)	3.5	-11.4	3.3	3.6	-11.9	2.7
B3P86/EPR-III	10.3	-23.3	-5.9	9.29 (0.8)	4.0	-14.1	3.4	6.0	-18.3	-0.9
B3P86/aug-cc-pVTZ-J	5.5	-15.5	-0.9	4.13 (0.7)	3.5	-11.4	3.3	3.6	-10.5	4.1
B3P86/ccJ-pVTZ	8.2	-20.3	-3.6	7.04 (0.8)	3.9	-13.3	3.4	4.4	-15.3	1.4
B3P86/pcJ-2	5.6	-15.9	-0.9	4.35 (0.7)	3.5	-11.6	3.4	3.6	-10.9	4.1
B97-2/TZVP	15.2	-32.7	-9.2	13.99 (1.0)	5.3	-18.7	4.8	10.6	-27.7	-4.2
B97-2/HIII-su3	8.2	-21.2	-1.8	6.85 (0.8)	4.3	-14.3	5.0	4.7	-16.2	3.2
B97-2/EPR-III	12.3	-28.1	-6.1	11.06 (0.9)	4.8	-17.0	5.0	7.8	-23.1	-1.1
B97-2/aug-cc-pVTZ-J	6.3	-18.9	0.3	4.54 (0.8)	4.2	-14.3	4.9	4.2	-13.9	5.3
B97-2/ccJ-pVTZ	10.4	-26.1	-4.1	9.06 (0.9)	4.9	-17.0	4.9	6.4	-21.1	0.9
B97-2/pcJ-2	7.6	-20.4	-0.8	6.16 (0.8)	4.2	-14.3	5.4	4.4	-15.4	4.2
M06-L/TZVP	42.0	32.4	46.8	-41.04 (0.7)	3.9	-8.7	5.8	47.1	37.4	51.8
M06-L/HIII-su3	40.3	30.6	46.2	-39.35 (0.7)	3.8	-8.7	6.8	45.4	35.6	51.2
M06-L/EPR-III	42.3	31.5	47.8	-41.36 (0.8)	3.9	-9.9	6.4	47.4	36.5	52.8
M06-L/aug-cc-pVTZ-J	36.0	25.7	42.3	-35.16 (0.7)	3.9	-9.4	7.1	41.1	30.7	47.3
M06-L/ccJ-pVTZ	41.8	33.5	47.0	-40.91 (0.7)	3.4	-7.5	6.1	46.9	38.5	52.0
M06-L/pcJ-2	45.8	36.8	51.0	-44.85 (0.7)	3.6	-8.0	6.1	50.9	41.8	56.0
B3LYP/TZVPg	4.6	-12.7	-0.2	3.28 (0.6)	3.2	-9.4	3.1	3.7	-7.7	4.8
B3P86/aug-cc-pVTZ-Jg	5.9	-14.7	-1.4	4.92 (0.6)	3.2	-9.8	3.5	3.2	-9.7	3.6

deviation larger than 5 Hz in magnitude. Four of them correspond to $HC(O) - X$ with $X = F$ (-12.7 Hz of deviation), CH_3 (-7.7 Hz), C_6H_5 (-6.3 Hz) and OCH_3 (-5.7 Hz). The remaining two largest deviations correspond to $cis-H(CN)C = CH(CN)$ (-9.4 Hz) and $HCH = \overline{CH}(CN)$ (-7.5 Hz, the coupled hydrogen is the overlined one). Shifted results have similar quality for all functional/basis set combinations. $\sigma^{(1)}$ ranges from 2.8 (B3LYP with HIII-su3, aug-cc-pVTZ-J, pcJ-2 or pcJ-3) to 5.4 Hz (PBE/TZVP). Additionally, M06-L functional yields reasonable results when an independent term ranging between -35 and -44 Hz is used. Five models yield $\sigma^{(rv)}$ values smaller than 4 Hz: B3P86 with HIII-su3, aug-cc-pVTZ-J and pcJ-2, B3LYP/TZVPg and B3P86/aug-cc-pVTZ-Jg. Again, the worst results are those of the B3LYP functional (excluding when the TZVP basis set is used) and those of TZVP basis set with PBE, B3P86 and B97-2 functionals.

Set-4 is the smaller data collection with only ten data points and includes couplings involving sp hybridized carbon atoms. This set ranges from 248 to 275 Hz, which represent the larger SSCC values of the whole data. However, seven experimental SSCCs have

a narrow range (from 248 to 253 Hz), and on the other hand, the experimental values could have large uncertainties.^[61] Therefore, it is not possible to draw definitive conclusions with this reduced and ill-conditioned set. Models with $\sigma^{(0)}$ smaller than 6 Hz are as follows: B97-2/HIII-su3 (4.6 Hz), B3P86/EPR-III (5.3 Hz), B3P86/ccJ-pVTZ (5.3 Hz), B97-2/pcJ-2 (5.4 Hz) and B97-2/pccJ-pVTZ (5.9 Hz). The worst results are those of M06-L functional ($\sigma^{(0)}$ between 73 and 81 Hz) and those of B3LYP functional when the largest basis sets are used ($\sigma^{(0)}$ between 18 and 28 Hz). However, when the calculated values are fitted to Eqn (1), best results are those of B3LYP functional ($\sigma^{(1)}$ between 4.1 and 4.4 Hz). The remaining functional/basis set combinations give slightly higher $\sigma^{(1)}$ deviations reaching 7.0 Hz for M06-L/pcJ-2.

The last data set (set-5) ranges from 154 to 206 Hz and contains 21 couplings that involve aromatic carbons. Results are close to those for set-3 (couplings with sp^2 -carbon atoms). The best fit corresponds to B3LYP/TZVPg and B3LYP/TZVP results ($\sigma^{(0)}$ of 2.4 and 2.5 Hz, respectively). However, TZVP and EPR-III basis sets yield worse results when using the remaining functionals. Other

Table 5. Statistical results (in hertz) for data set-4 (*sp* hybridized carbon atoms) using the indicated functional/basis set. γ -intercept ($\sigma^{(1)}$) for fits to Eqn (1) and its standard deviation (between parentheses) are given

Func./basis set	Original values			Shifted using Eqn (1)				5 Hz of rovib. contr.		
	$\sigma^{(0)}$	min ⁽⁰⁾	max ⁽⁰⁾	$a^{(1)}$	$\sigma^{(1)}$	min ⁽¹⁾	max ⁽¹⁾	$\sigma^{(rv)}$	min ^(rv)	max ^(rv)
PBE/TZVP	12.9	-24.8	-4.3	11.05 (1.8)	5.6	-13.8	6.8	8.5	-19.8	0.7
PBE/HIII-su3	6.1	-12.5	8.0	-1.94 (1.8)	5.7	-14.5	6.0	9.3	-7.5	13.0
PBE/EPR-III	8.1	-20.1	0.7	5.33 (1.8)	5.8	-14.8	6.0	5.8	-15.1	5.7
PBE/aug-cc-pVTZ-J	6.7	-11.6	10.0	-3.13 (1.9)	5.9	-14.7	6.9	10.4	-6.6	15.0
PBE/ccJ-pVTZ	6.1	-16.2	5.4	1.01 (1.9)	6.0	-15.2	6.4	7.3	-11.2	10.4
PBE/pcJ-2	7.3	-10.7	11.0	-4.14 (1.9)	5.9	-14.8	6.9	11.3	-5.7	16.0
B3LYP/TZVP	9.5	-0.9	14.6	-8.03 (1.3)	4.3	-8.9	6.6	14.4	4.1	19.6
B3LYP/HIII-su3	26.6	16.1	30.9	-24.91 (1.3)	4.1	-8.9	6.0	31.8	21.1	35.9
B3LYP/EPR-III	18.5	7.4	22.8	-17.05 (1.3)	4.3	-9.7	5.7	23.6	12.4	27.8
B3LYP/aug-cc-pVTZ-J	27.8	16.7	32.6	-26.07 (1.4)	4.3	-9.4	6.5	33.0	21.7	37.6
B3LYP/ccJ-pVDZ	22.7	11.6	27.2	-21.10 (1.4)	4.3	-9.5	6.1	27.8	16.6	32.2
B3LYP/ccJ-pVTZ	23.1	11.8	27.7	-21.56 (1.4)	4.4	-9.8	6.2	28.3	16.8	32.7
B3LYP/ccJ-pVQZ	26.7	15.7	31.3	-25.01 (1.4)	4.3	-9.3	6.3	31.9	20.7	36.3
B3LYP/pcJ-2	28.1	17.0	32.9	-26.38 (1.4)	4.3	-9.3	6.6	33.4	22.0	37.9
B3LYP/pcJ-3	27.2	16.4	31.9	-25.52 (1.3)	4.2	-9.1	6.4	32.4	21.4	36.9
B3P86/TZVP	12.1	-21.6	-4.8	10.60 (1.5)	4.7	-11.0	5.8	7.5	-16.6	0.2
B3P86/HIII-su3	6.7	-6.4	9.8	-4.63 (1.4)	4.6	-11.0	5.2	11.1	-1.4	14.8
B3P86/EPR-III	5.3	-13.9	2.8	2.11 (1.5)	4.8	-11.8	4.9	5.7	-8.9	7.8
B3P86/aug-cc-pVTZ-J	8.1	-5.4	12.0	-6.23 (1.5)	4.8	-11.6	5.7	12.8	-0.4	17.0
B3P86/ccJ-pVTZ	5.3	-10.0	7.3	-1.98 (1.5)	4.9	-11.9	5.4	8.8	-5.0	12.3
B3P86/pcJ-2	7.8	-5.6	11.6	-5.87 (1.5)	4.8	-11.4	5.8	12.4	-0.6	16.6
B97-2/TZVP	9.9	-19.5	-2.5	8.21 (1.5)	4.8	-11.3	5.7	5.9	-14.5	2.5
B97-2/HIII-su3	4.6	-10.9	5.3	-0.67 (1.4)	4.6	-11.6	4.6	7.5	-5.9	10.3
B97-2/EPR-III	8.6	-19.4	-2.1	6.60 (1.6)	5.0	-12.8	4.5	5.3	-14.4	2.9
B97-2/aug-cc-pVTZ-J	6.4	-8.7	8.8	-3.86 (1.6)	5.0	-12.6	5.0	10.6	-3.7	13.8
B97-2/ccJ-pVTZ	5.9	-15.8	1.7	2.86 (1.6)	5.1	-12.9	4.5	5.5	-10.8	6.7
B97-2/pcJ-2	5.4	-10.8	6.9	-1.86 (1.6)	5.0	-12.6	5.1	8.8	-5.8	11.9
M06-L/TZVP	81.1	63.0	86.2	-76.74 (2.0)	6.3	-13.8	9.5	86.4	68.0	91.2
M06-L/HIII-su3	80.8	65.5	85.1	-76.47 (1.7)	5.3	-10.9	8.7	86.0	70.5	90.1
M06-L/EPR-III	77.7	58.5	84.2	-73.40 (2.1)	6.6	-14.9	10.8	82.9	63.5	89.2
M06-L/aug-cc-pVTZ-J	72.8	57.6	79.3	-68.84 (1.8)	5.6	-11.2	10.4	78.0	62.6	84.3
M06-L/ccJ-pVTZ	77.2	59.2	83.1	-73.04 (2.0)	6.2	-13.8	10.1	82.5	64.2	88.1
M06-L/pcJ-2	77.3	56.7	83.7	-73.05 (2.2)	7.0	-16.3	10.6	82.6	61.7	88.7
B3LYP/TZVPg	8.2	-1.8	13.4	-6.72 (1.3)	4.2	-8.5	6.7	13.0	3.2	18.4
B3P86/aug-cc-pVTZ-Jg	6.4	-6.7	9.9	-4.24 (1.4)	4.6	-10.9	5.7	10.8	-1.7	14.9

results with $\sigma^{(0)}$ smaller than 6 Hz are those of B3P86/aug-cc-pVTZ-J ($\sigma^{(0)} = 3.9$ Hz), B3P86/pcJ-2 (4.0 Hz), B3LYP/EPR-III (4.6 Hz), B97-2/aug-cc-pVTZ-J (4.8 Hz), B3P86/aug-cc-pVTZ-Jg (4.8 Hz) and B3P86/HIII-su3 (5.1 Hz). Again, M06-L functional produces the worst results ($\sigma^{(0)}$ from 35 to 44 Hz). B3LYP/TZVPg results only present one deviation larger than 5 Hz in magnitude. This is that of $^1J_{C_{ortho}-H}$ in $C_6H_5F(o)$ (7.1 Hz). It should be noted that while most of the SSCCs calculated at B3LYP/TZVPg are smaller than the experimental ones, the coupling for C_6H_5F is 7 Hz larger (this deviation can be identified easily in Fig. 1). This large and positive deviation contrasts with the small one (0.1 Hz with B3LYP/TZVPg) obtained for $C_6H_3F_3$ molecule. This leads us to suspect that the experimental value could be incorrect. The shifted couplings improve their performance and yield similar results for all functional/basis set combinations with $\sigma^{(1)}$ of 2.1–2.4 Hz (3.2–4.0 for the M06-L functional). The calculated values corrected with 5 Hz of rovibrational contribution present results similar to those indicated previously for the other sets. Several models yield $\sigma^{(rv)}$ values smaller than 3 Hz: PBE, B3P86 and B97-2 with aug-cc-pVTZ-

J and pcJ-2, B3P86 and B97-2 with HIII-su3, B3P86/ccJ-pVTZ and B3P86/aug-cc-pVTZ-g. B3LYP results and those obtained with the TZVP yield large $\sigma^{(rv)}$ values between 7 and 15 Hz, excepting B3LYP/TZVP (4.6 Hz).

Figures 2 and 3 show the deviations $^1J_{CH}^{Calc} - ^1J_{CH}^{Exp}$ against the functional/basis set used for the calculation of the SSCC (Fig. 2) or against the number of contracted basis functions (Fig. 3). Calculated values $^1J_{CH}^{Calc}$ in Fig. 3 correspond to those obtained with B3LYP functional and the indicated basis set. These figures were represented for four well-known molecules: CH_4 , $CH_2 = CH_2$, $HC \equiv CH$ and C_6H_6 , one of each type of coupling. Figures for all studied molecules are presented in the Supporting Information. In Fig. 2, different symbols have been used for each functional, and some interesting trends are observed. The results calculated with B3LYP and M06-L functional are, in general, larger than the experimental ones while the remaining functionals yield smaller SSCCs. The values calculated with TZVP basis set are, within each functional, the smallest one. Roughly, the deviations $^1J_{CH}^{Calc} - ^1J_{CH}^{Exp}$ for each approach follow the same pattern independently of the

Table 6. Statistical results (in hertz) for data set-5 (aromatic carbon atoms) using the indicated functional/basis set. Y-intercept ($\sigma^{(1)}$) for fits to Eqn (1) and its standard deviation (between parentheses) are given

Func./basis set	Original values			Shifted using Eqn (1)				5 Hz of rovib. contr.		
	$\sigma^{(0)}$	min ⁽⁰⁾	max ⁽⁰⁾	$\sigma^{(1)}$	$\sigma^{(1)}$	min ⁽¹⁾	max ⁽¹⁾	$\sigma^{(rv)}$	min ^(rv)	max ^(rv)
PBE/TZVP	14.1	-18.2	-6.1	13.61 (0.5)	2.3	-4.6	7.5	9.1	-13.2	-1.1
PBE/HIII-su3	7.1	-9.4	0.7	6.62 (0.5)	2.1	-2.8	7.3	2.7	-4.4	5.7
PBE/EPR-III	11.0	-13.8	-3.0	10.48 (0.5)	2.2	-3.3	7.5	6.0	-8.8	2.0
PBE/aug-cc-pVTZ-J	6.1	-8.5	1.8	5.60 (0.5)	2.1	-2.9	7.4	2.2	-3.5	6.8
PBE/ccJ-pVTZ	8.4	-10.7	-0.4	7.93 (0.5)	2.2	-2.8	7.5	3.7	-5.7	4.6
PBE/pcJ-2	5.0	-7.4	3.0	4.43 (0.5)	2.1	-2.9	7.4	2.2	-2.4	8.0
B3LYP/TZVP	2.5	-4.5	6.9	1.08 (0.5)	2.3	-3.4	8.0	4.6	0.5	11.9
B3LYP/HIII-su3	8.7	5.2	15.8	-8.24 (0.5)	2.2	-3.0	7.6	13.7	10.2	20.8
B3LYP/EPR-III	4.6	1.2	11.7	-4.00 (0.5)	2.2	-2.8	7.7	9.5	6.2	16.7
B3LYP/aug-cc-pVTZ-J	9.7	6.3	16.8	-9.19 (0.5)	2.2	-2.9	7.6	14.7	11.3	21.8
B3LYP/ccJ-pVDZ	6.5	2.9	13.9	-5.90 (0.5)	2.3	-2.9	8.0	11.4	7.9	18.9
B3LYP/ccJ-pVTZ	7.0	3.6	14.2	-6.50 (0.5)	2.2	-2.9	7.7	12.0	8.6	19.2
B3LYP/ccJ-pVQZ	9.1	5.7	16.3	-8.64 (0.5)	2.2	-2.9	7.7	14.1	10.7	21.3
B3LYP/pcJ-2	10.1	6.8	17.3	-9.66 (0.5)	2.2	-2.9	7.7	15.2	11.8	22.3
B3LYP/pcJ-3	9.3	6.0	16.5	-8.88 (0.5)	2.2	-2.9	7.6	14.4	11.0	21.5
B3P86/TZVP	13.6	-18.4	-5.2	13.08 (0.5)	2.4	-5.3	7.9	8.6	-13.4	-0.2
B3P86/HIII-su3	5.1	-7.4	3.0	4.51 (0.5)	2.1	-2.9	7.5	2.2	-2.4	8.0
B3P86/EPR-III	8.5	-11.5	-0.4	7.98 (0.5)	2.2	-3.5	7.6	3.8	-6.5	4.6
B3P86/aug-cc-pVTZ-J	3.9	-5.9	4.3	3.21 (0.5)	2.1	-2.7	7.5	2.8	-0.9	9.3
B3P86/ccJ-pVTZ	6.3	-8.6	1.8	5.78 (0.5)	2.2	-2.8	7.6	2.3	-3.6	6.8
B3P86/pcJ-2	4.0	-6.1	4.2	3.38 (0.5)	2.1	-2.7	7.5	2.7	-1.1	9.2
B97-2/TZVP	12.0	-16.7	-3.7	11.48 (0.5)	2.3	-5.2	7.8	7.0	-11.7	1.3
B97-2/HIII-su3	6.8	-9.7	1.3	6.28 (0.5)	2.2	-3.4	7.6	2.6	-4.7	6.3
B97-2/EPR-III	10.8	-14.7	-2.8	10.28 (0.5)	2.2	-4.4	7.4	5.9	-9.7	2.2
B97-2/aug-cc-pVTZ-J	4.8	-7.1	3.2	4.19 (0.5)	2.1	-3.0	7.3	2.3	-2.1	8.2
B97-2/ccJ-pVTZ	8.7	-12.4	-0.8	8.25 (0.5)	2.2	-4.2	7.4	4.0	-7.4	4.2
B97-2/pcJ-2	6.3	-8.6	1.6	5.77 (0.5)	2.1	-2.9	7.4	2.3	-3.6	6.6
M06-L/TZVP	44.5	37.3	54.0	-43.22 (0.9)	4.0	-5.9	10.8	49.6	42.3	59.0
M06-L/HIII-su3	39.9	32.9	48.2	-38.71 (0.9)	3.9	-5.8	9.5	45.0	37.9	53.2
M06-L/EPR-III	42.4	35.9	50.5	-41.18 (0.8)	3.7	-5.2	9.3	47.5	40.9	55.5
M06-L/aug-cc-pVTZ-J	35.1	28.4	44.0	-34.06 (0.9)	4.0	-5.7	10.0	40.2	33.4	49.0
M06-L/ccJ-pVTZ	41.4	34.7	50.3	-40.21 (0.9)	3.9	-5.6	10.1	46.5	39.7	55.3
M06-L/pcJ-2	45.8	39.7	52.2	-44.55 (0.7)	3.2	-4.8	7.7	50.9	44.7	57.2
B3LYP/TZVPg	2.4	-3.4	7.1	1.00 (0.5)	2.2	-2.5	8.1	4.6	1.6	12.1
B3P86/aug-cc-pVTZ-Jg	4.8	-6.8	3.3	4.24 (0.5)	2.1	-2.6	7.5	2.2	-1.8	8.3

molecule (see Supporting Information). In Fig. 3, we investigate the convergence of this SSCC against the number of basis functions. This figure shows (see also the Supporting Information) that the largest basis sets (ccJ-pVQZ and pcJ-3) do not introduce any improvement with respect to the smaller ones. Considering a possible convergence with the size of the basis set, the medium-large basis sets aug-cc-pVTZ-J, pcJ-2 and the HIII-su3 seem to yield good results close to those of the largest ones. The performance of the ccJ-pVDZ and ccJ-pVTZ is quite similar in spite of their different sizes, and compared with the large basis sets, they yield slightly smaller SSCCs. It should be noted that the smaller and inexpensive TZVP basis set gives the smallest calculated values for each functional. Moreover, when it is combined with B3LYP functional, which usually overestimates the calculated values, results present the smallest deviation against the experimental. A physical explanation for the low values calculated with TZVP basis set is its incorrect description of the densities at the nucleus. Thus, in the methane molecule, the nuclear densities for the carbon

and for the hydrogen amount between 125.9 and 126.2 a.u. and between 0.4877 and 0.4940 a.u., respectively, when calculated with B3LYP and all basis sets, except the EPR-III and TZVP. For these last basis sets, the densities amount 123.1 and 121.9 u.a. for carbon and 0.485 and 0.437 u.a. for hydrogen. These low densities obtained specially with the TZVP increase significantly when one tight s function is added to the carbon and to the hydrogens. In this case, the densities increase to 124.6 and 0.475 u.a. for carbon and hydrogen, respectively, and $^1J_{CH}^{Calc}$ increase in 12 Hz. It is worth noting that the correct description of nuclear densities is important only for the FC contribution, which, for coupling constants studied in this work, is dominant.

Fitted coupling constants obtained using Eqn (1) show results for different functional/basis set combinations that are qualitatively similar. $\sigma^{(1)}$ and $\sigma^{(2)}$ values for all the approaches, excepting for M06-L results, fall within a narrow interval (see Tables 2–6 and Supporting Information). Another interesting aspect is that differences $^1J_{CH}^{Calc} - ^1J_{CH}^{Exp}$ calculated with different functional/basis

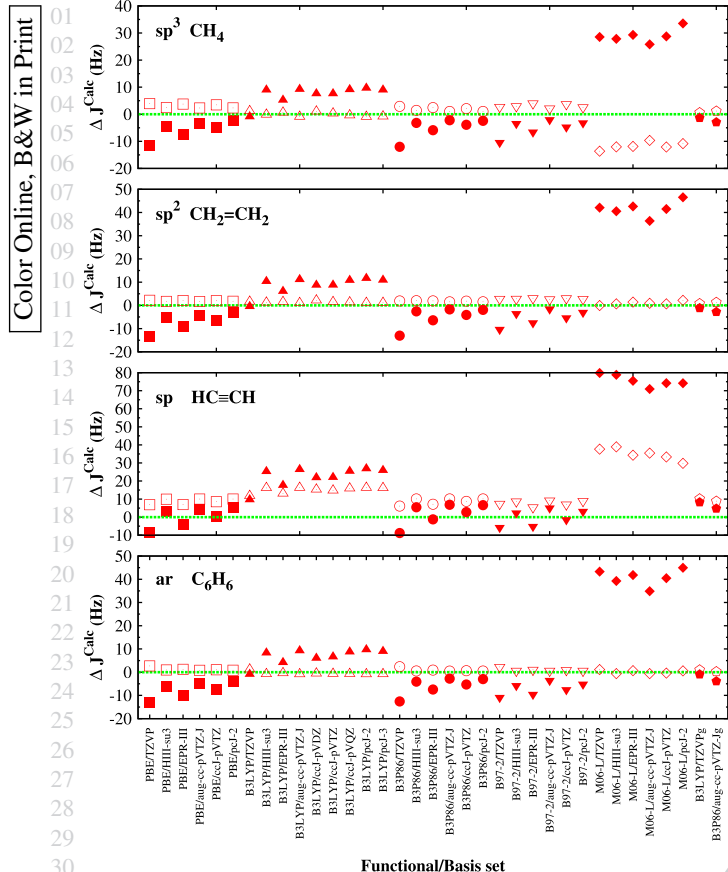


Figure 2. Deviation $\Delta J^{\text{Calc}} = {}^1J_{\text{CH}}^{\text{Calc}} - {}^1J_{\text{CH}}^{\text{Exp}}$ against the indicated functional/basis set approach for four representative molecules. Original calculated values (solid symbols) and those shifted (open symbols) using $a^{(1)}$ independent terms obtained for the whole set (see Table 2).

sets present large dispersion. However, the deviations, ${}^1J_{\text{CH}}^{\text{Shifted}} - {}^1J_{\text{CH}}^{\text{Exp}}$, where ${}^1J_{\text{CH}}^{\text{Shifted}} = a^{(1)} + {}^1J_{\text{CH}}^{\text{Calc}}$, are much more homogeneous within a given coupling independently of the used functional/basis set. These last deviations were used to detect wrong or systematic trends within DFT results. Molecules that present the largest average deviation are shown in Table 7. The average is carried out over 29 different approaches (M06-L results were excluded) with the couplings shifted using optimized independent term of Eqn (1) over each respective set of couplings types, that is, sp^3 , sp^2 , Only values with average deviation larger than 5 Hz are presented in Table 7. root-mean-square σ values for those average deviations, shown in parentheses in Table 7, are small because of the narrow dispersion indicated earlier. M06-L results were excluded owing to their larger deviations; however, their inclusion does not change qualitatively the results presented in Table 7. The deviations for some of the best functional/basis set combinations are also shown in Table 7. Some of these couplings could be defined as difficult or ill-conditioned couplings, which are problematic for DFT calculations and could be a good test for future calculations. The fact that fitted couplings present a similar quality notwithstanding the used functional/basis set is not surprising. Previous DFT studies show that the substituent effects on coupling constants^[11,62] and chemical shifts^[63,64] are predicted correctly; that is, the qualitative trends of these effects are well reproduced although the calculated values vary more with experiments.

Table 7 deserves further comments. For SSCCs with sp^3 -carbon, the only value that deviates more than 5 Hz in magnitude corresponds to $\text{CH}_2\text{F}(\text{CN})$ (−7.1 Hz of deviation). This is a molecule with electronegative substituents with lone pair electrons (F) and a triple bond (cyano group) attached to the coupled carbon atom. For SSCCs involving sp^2 -carbon, we detect two values with larger deviations. One of them is formyl fluoride (−12.3 Hz of average deviation), where the coupling carbon belongs to a carbonyl group like in acetaldehyde, formaldehyde and benzaldehyde, which also show large average deviations of −3.9, 3.5 and −2.6 Hz, respectively. The second largest average deviation (−6.7 Hz) corresponds to $\text{cis-}H(\text{CN})\text{C}=\text{CH}(\text{CN})$, again a molecule with cyano groups. For the sp -carbon set, two molecules present deviations larger than 5 Hz: hydrogen cyanide (−10.9 Hz) and fluoroacetylene (5.8 Hz). Despite being well-studied molecules, they present large deviations. These results should be viewed in the context of reduced and ill-conditioned data set (see the previous paragraphs) that may bias the fitted values in the wrong direction. When the carbon involved in the coupling is aromatic, only the values for the *ortho*- ${}^1J_{\text{CH}}$ in fluorobenzene deviate more than 5 Hz; here, it is 7.6 Hz (see aforementioned comments about this result).

A summary of results using the original group of calculated SSCCs and that obtained after subtracting a constant rovibrational contribution of 5 Hz is presented in Table 8. In this table, the results for set-5 (sp involved carbon) were not included owing to the discrepancies indicated earlier. In order to better visualize the results, the σ values were presented using different colors. The values with σ between 4 and 5 Hz or smaller (in this last case, the figures are indicated) are in green; σ values between 5 and 6 Hz are in blue; σ values between 6 and 7 Hz are in red; σ deviations between 7 and 10 Hz are not indicated; and σ larger than 10 Hz are presented. This classification allows us to distinguish four groups of models (functional/basis set):

- (1) Models that yield σ deviations that are low for both groups of results. These are B3LYP/TZVPg, B3P86/aug-cc-pVTZ-Jg, B3LYP/TZVP and B3P86/aug-cc-pVTZ-J.
- (2) Models that yield good results when a rovibrational contribution of 5 Hz is considered. But, in general, they do not yield good σ deviations for the original (non-scaled) group of SSCCs. These models are PBE, B3P86 and B97-2 with HII-su3, pcJ-2 and PBE/aug-cc-pVTZ-J, B3P86/ccJ-pVTZ and B97-2/aug-cc-pVTZ-J.
- (3) Few models give good results for set-2 without considering the rovibrational contributions. These models could also give reasonable results for set-3 and set-5. They are mainly B3LYP with EPR-III, ccJ-pVDZ and ccJ-pVTZ.
- (4) A large set of models with worse results, mainly with σ deviations larger than 7 Hz. These four groups are separated in Table 7 by a blank space.

The overestimated results obtained with the M06-L functional could be attributed to the fact that it does not involve Hartree–Fock exchange (E_{x}^{HF}). Test results obtained using the M062X (54% of E_{x}^{HF}) and M06HF (100% of E_{x}^{HF}) functionals seem to yield smaller values. Thus, for methane, the ${}^1J_{\text{CH}}^{\text{FC}}$ value obtained with M06-L/TZVP is 140.8 Hz, while with M062X/TZVP and M06HF/TZVP, values are 126.9 and 91.6 Hz, respectively. It should be noted, however, that the PBE functional used also in this work does not involve E_{x}^{HF} and the results obtained are not overestimated.

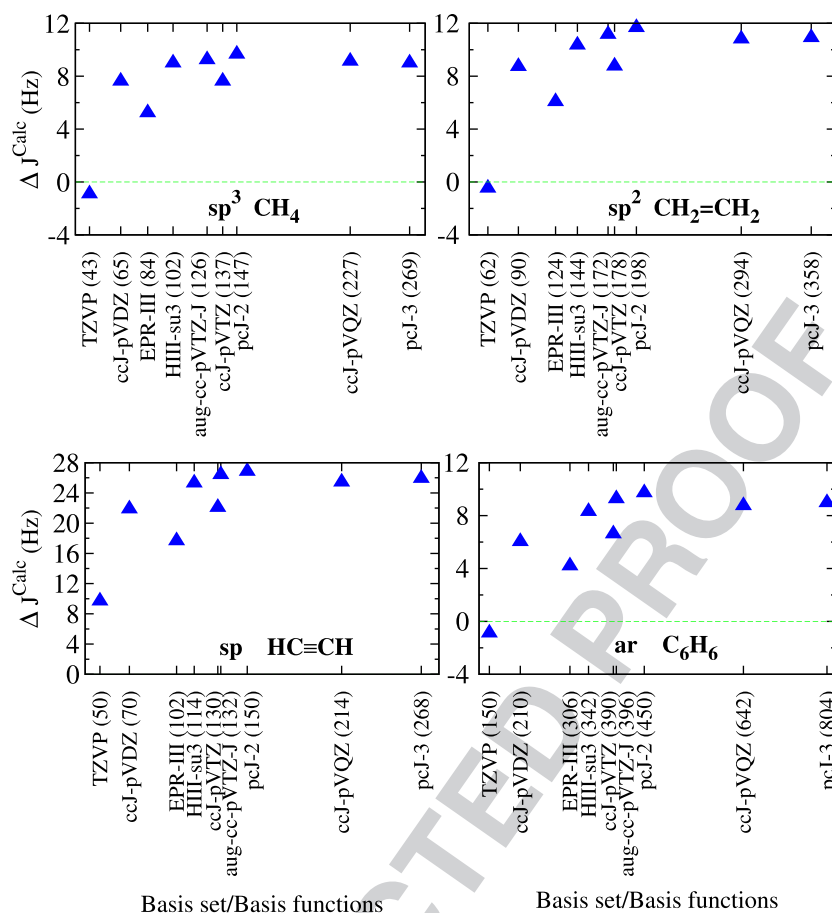


Figure 3. Deviation $\Delta J^{\text{Calc}} = J_{\text{CH}}^{\text{Calc}} - J_{\text{CH}}^{\text{Exp}}$ against the number of contracted basis functions for four representative molecules. B3LYP functional was used.

Table 7. Deviations $J_{\text{CH}}^{\text{Shifted}} - J_{\text{CH}}^{\text{Exp}}$ for some representative results^a. Last column corresponds to the average deviation over the 29 calculations for the indicated molecule

Molecule	Type	$J_{\text{CH}}^{\text{Exp}}$	B3LYP/TZVP	B3LYP/TZVPg	B3P86/aug-cc-pVTZ	B3P86/aug-cc-pVTZg	Average ^b
<chem>FH2C-C#N</chem>	sp ³	166.0	-6.9	-6.5	-6.9	-7.0	-7.1 (0.6)
<chem>N#C-CH=CH-N#C</chem>	sp ²	184.0	-5.6	-6.2	-6.3	-6.6	-6.7 (0.6)
<chem>F-C(=O)H</chem>	sp ²	267.0	-13.5	-9.4	-11.4	-9.8	-12.3 (3.8)
<chem>H-C#N</chem>	sp	269.0	-8.9	-8.5	-11.6	-11.2	-10.9 (2.1)
<chem>HC#CF</chem>	sp	275.5	6.6	6.7	5.7	5.7	5.8 (0.7)
<chem>c1ccccc1F</chem>	ar	155.0	8.0	8.1	7.5	7.5	7.6 (0.2)

^aOnly couplings with average deviations larger than 5 Hz in magnitude are presented.

^b σ deviations for these average values, shown in parentheses, are presented.

Table 8. Summary of σ deviations^a (hertz) for functional/basis set models and for original calculated group and that obtained assuming 5 Hz of rovibrational contribution

Func./Basis set	Original group				5 Hz of rovib. cont.			
	Set-1 (Whole)	Set-2 (sp^3)	Set-3 (sp^2)	Set-5 (Arom)	Set-1 (Whole)	Set-2 (sp^3)	Set-3 (sp^2)	Set-5 (Arom)
B3LYP/TZVPg	4–5	4–5	4–5	2.4	5–6	2.3	3.7	4–5
B3P86/aug-cc-pVTZ-Jg	5–6	6–7	5–6	4–5	4–5	2.5	3.2	2.2
B3LYP/TZVP	5–6	5–6	5–6	2.5	5–6	2.5	4–5	4–5
B3P86/aug-cc-pVTZ-J	5–6	6–7	5–6	3.9	4–5	2.4	3.6	2.8
PBE/HIII-su3					5–6	4–5	5–6	2.7
PBE/aug-cc-pVTZ-J				6–7	4–5	4–5	4–5	2.2
PBE/pcJ-2	6–7			4–5	4–5	3.2	4–5	2.2
B3P86/HIII-su3			6–7	5–6	4–5	3.1	3.6	2.2
B3P86/ccJ-pVTZ				6–7	4–5	3.8	4–5	2.3
B3P86/pcJ-2	5–6	6–7	5–6	4–5	4–5	2.5	3.6	2.7
B97-2/HIII-su3				6–7	4–5	4–5	4–5	2.6
B97-2/aug-cc-pVTZ-J	6–7		6–7	4–5	4–5	3.0	4–5	2.3
B97-2/pcJ-2				6–7	4–5	4–5	4–5	2.3
B3LYP/EPR-III		2.7	5–6	4–5	> 10			
B3LYP/ccJ-pVDZ		4–5	6–7	6–7	> 10		> 10	> 10
B3LYP/ccJ-pVTZ		4–5			> 10		> 10	> 10
PBE/ccJ-pVTZ		> 10	> 10		5–6	5–6	6–7	3.7
B3P86/EPR-III	6–7	> 10	> 10		5–6	5–6	6–7	3.8
B97-2/ccJ-pVTZ		> 10	> 10		5–6	5–6	6–7	4–5
PBE/EPR-III	> 10	> 10	> 10	> 10				6–7
B3LYP/HIII-su3	> 10	5–6			> 10	> 10	> 10	> 10
B3LYP/aug-cc-pVTZ-J	> 10	6–7	> 10		> 10	> 10	> 10	> 10
B3LYP/ccJ-pVQZ	> 10	6–7			> 10	> 10	> 10	> 10
B3LYP/pcJ-3	> 10	6–7			> 10	> 10	> 10	> 10
B97-2/TZVP	> 10	> 10	> 10	> 10		> 10	> 10	6–7
B97-2/EPR-III	> 10	> 10	> 10	> 10	6–7			5–6
PBE/TZVP	> 10	> 10	> 10	> 10	> 10	> 10	> 10	
B3LYP/pcJ-2	> 10	> 10	> 10	> 10	> 10	> 10	> 10	> 10
B3P86/TZVP	> 10	> 10	> 10	> 10	> 10	> 10	> 10	
M06-L/TZVP	> 10	> 10	> 10	> 10	> 10	> 10	> 10	> 10
M06-L/HIII-su3	> 10	> 10	> 10	> 10	> 10	> 10	> 10	> 10
M06-L/EPR-III	> 10	> 10	> 10	> 10	> 10	> 10	> 10	> 10
M06-L/aug-cc-pVTZ-J	> 10	> 10	> 10	> 10	> 10	> 10	> 10	> 10
M06-L/ccJ-pVTZ	> 10	> 10	> 10	> 10	> 10	> 10	> 10	> 10
M06-L/pcJ-2	> 10	> 10	> 10	> 10	> 10	> 10	> 10	> 10

^a Values between 4 and 5 Hz or smaller (in green), between 5 and 6 Hz (blue) and between 6 and 7 Hz (red). Values larger than 10 Hz are indicated and those not shown correspond to values between 7 and 10 Hz.

Conclusions

A large collection of one-bond carbon–hydrogen NMR coupling constants was calculated at different DFT levels and compared with experimental values in order to detect the main trends and to search for the best choice of functional and basis set combination. Five density functionals and nine atomic basis sets were tested in the calculation of 88 $^1J_{CH}$ values. Regression analysis was used as a basic and appropriate methodology for this type of comparative study.

Directly calculated SSCCs and those corrected with shifting and/or scaling factors for each model (functional/basis set) were compared with experimental values. Within the shifting approach, a particular case is to consider a fixed rovibrational contribution, a reasonable value for it could be 5 Hz, that was subtracted from the experimental or added to the calculated values.

When the calculated SSCCs are modified with shifting factors (independent term $a^{(1)}$ in Eqn (1)) all results improve significantly presenting $\sigma^{(1)}$ values between 4.0 and 6.5 Hz for the whole set of SSCCs, excluding M06-L results. This later functional yields $\sigma^{(1)}$ deviations between 12 and 15 Hz. The $a^{(1)}$ corrections are negative (the calculated values are overestimated) for M06-L results (between –35 and –44 Hz) and for B3LYP (between –4.6 and –10.6 Hz) excepting B3LYP/TZVP and B3LYP/TZVPg that present a value

for $a^{(1)}$ of 2 Hz. For the remaining models, $a^{(1)}$ values are positive between 3.2 and 15.6 Hz.

Considering the original calculated group (unfitted) and that including 5 Hz of rovibrational contribution, one can detect a small set of models that performs properly for both groups of SSCCs. These are B3LYP/TZVPg, B3P86/aug-cc-pVTZ-Jg, B3LYP/TZVP and B3P86/aug-cc-pVTZ-J (see Table 8). A second group of models with PBE, B3P86 and B97-2 functionals in combination with HIII-su3, and pcJ-2 basis sets and the models PBE/aug-cc-pVTZ-J, B3P86/ccJ-pVTZ and B97-2/aug-cc-pVTZ-J yield good results when the indicated rovibrational contribution is considered. Models with B3LYP and EPR-III, ccJ-pVDZ and ccJ-pVTZ yield satisfactory results mainly for the original set-2 (sp^3 involved carbons). The remaining models that seem to work worse irrespective of that rovibrational contributions are considered (see Table 8). It should be stressed the incorrect performance of M06-L functional for these kinds of coupling constants.

Popular B3LYP functional overestimates the calculated coupling constants, overestimation that increases when the rovibrational contributions are included. On the other hand, TZVP basis set, the smallest one used in this work, gives for any functional the lower calculated values. Therefore, the combination of those opposite effects in the B3LYP/TZVP model yields good calculated values when compared with the experimental. This agreement

with the experimental values for the model B3LYP/TZVP can be attributed to error cancellation.

It is also important to stress, as observed in the previous works,^[1,65] that for lone-pair bearing electronegative substituents, $^1J_{CH}$ SSCC calculations are a difficult task for DFT methods. A similar assertion seems to hold for substituents involving triple bonds.

As a final conclusion, for calculating $^1J_{CH}$ SSCCs, we recommend using B3P86 functional in combination with aug-cc-pVTZ-J basis set when rovibrational contributions of 5 Hz are considered or, alternatively, the use of the shifting constants $a^{(1)}$ presented in Tables 2–6.

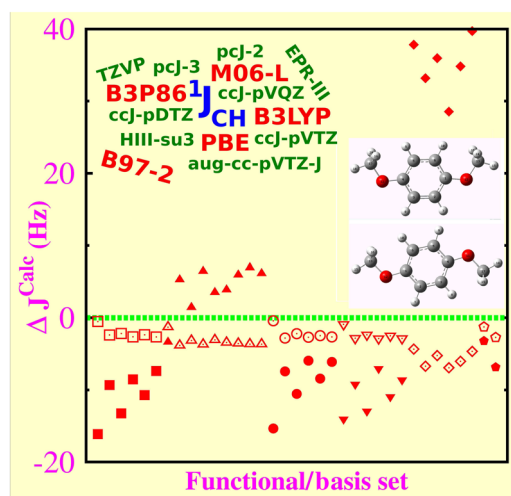
Acknowledgements

The financial supports of the following organizations are gratefully acknowledged: Dirección General de Enseñanza Superior e Investigación Científica of Spain (DGESIC), projects: CTQ2010-19232 and CTQ2010-17338 (J. M. G. V. and J. S. F.); Comunidad de Madrid, project S2009/ENE-1743 (J. S. F.); Spanish Agency of International Co-operation, project: A1/035856/11 (J. M. G. V., J. S. F., RS and R. C. O.); UBACYT, project: X 047 (R. H. C.) and CONICET, project: PIP 0369 (R. H. C.). Computer time provided by the Centro de Computación Científica of Universidad Autónoma de Madrid is gratefully acknowledged.

References

- [1] T. Helgaker, M. Jaszuński, M. Pecul. *Prog. Nucl. Magn. Reson. Spectrosc.* **2008**, *53*, 249.
- [2] L. B. Krivdin, R. H. Contreras. *Ann. Repts. NMR Spectrosc.* **2007**, *61*, 133.
- [3] D. Cremer, J. Grafenstein. *Phys. Chem. Chem. Phys.* **2007**, *9*, 2791.
- [4] J. Vaara. *Phys. Chem. Chem. Phys.* **2007**, *9*, 5399.
- [5] M. Bühl, T. van Mourik. *Wiley Interdisciplinary Reviews: Computational Molecular Science* **2011**, *1*, 634.
- [6] V. Sychrovsky, J. Grafenstein, D. Cremer. *J. Chem. Phys.* **2000**, *113*, 3530.
- [7] T. Helgaker, M. Watson, N. C. Handy. *J. Chem. Phys.* **2000**, *113*, 9402.
- [8] P. Lantto, J. Vaara, T. Helgaker. *J. Chem. Phys.* **2002**, *117*, 5998.
- [9] S. N. Maximoff, J. E. Peralta, V. Barone, G. E. Scuseria. *J. Chem. Theory Comput.* **2005**, *1*, 541.
- [10] T. W. Keal, T. Helgaker, P. Salek, D. J. Tozer. *Chem. Phys. Lett.* **2006**, *425*, 163.
- [11] A. Cunha Neto, F. P. dos Santos, R. H. Contreras, R. Rittner, C. F. Tormena. *J. Phys. Chem.* **2008**, *112*, 11956.
- [12] J. E. Peralta, G. E. Scuseria, J. R. Cheeseman, M. J. Frisch. *Chem. Phys. Lett.* **2003**, *375*, 452.
- [13] R. Suardiá, C. Pérez, R. Crespo-Otero, J. M. García de la Vega, J. San Fabián. *J. Chem. Theory Comput.* **2008**, *4*, 448.
- [14] A. Cunha Neto, F. P. dos Santos, A. S. Paula, C. F. Tormena, R. Rittner. *Chem. Phys. Lett.* **2008**, *454*, 129.
- [15] A. D. Becke. *J. Chem. Phys.* **1993**, *98*, 5648.
- [16] C. Lee, W. Yang, R. G. Parr. *Physical Rev. B.* **1988**, *37*, 785.
- [17] J. P. Perdew, K. Burke, M. Ernzerhof. *Phys. Rev. Lett.* **1996**, *77*, 3865.
- [18] J. P. Perdew, K. Burke, M. Ernzerhof. *Phys. Rev. Lett.* **1997**, *78*, 1396.
- [19] P. J. Wilson, T. J. Bradley, D. J. Tozer. *J. Chem. Phys.* **2001**, *115*, 9233.
- [20] T. W. Keal, D. J. Tozer. *J. Chem. Phys.* **2005**, *123*, 121103.
- [21] A. Schäfer, H. Horn, R. Ahlrichs. *J. Chem. Phys.* **1992**, *97*, 2571.
- [22] A. Schäfer, C. Huber, R. Ahlrichs. *J. Chem. Phys.* **1994**, *100*, 5829.
- [23] T. Helgaker, O. B. Lutnæs, M. Jaszuński. *J. Chem. Theory Comput.* **2007**, *3*, 86.
- [24] W. E. Richter, T. C. Rozada, E. A. Basso, R. M. Pontes, G. F. Gauze. *Comp. Theor. Chem.* **2011**, *964*, 116.
- [25] A. L. Esteban, E. Diez, M. P. Galache, J. San Fabián, J. Casanueva, R. H. Contreras. *Mol. Phys.* **2010**, *108*, 583–595.
- [26] Y. Zhao, D. G. Truhlar. *J. Chem. Phys.* **2006**, *125*, 194101.
- [27] Y. Zhao, D. G. Truhlar. *Acc. Chem. Res.* **2008**, *41*, 157.
- [28] Y. Zhao, D. G. Truhlar. *J. Phys. Chem. A* **2008**, *112*, 6794.
- [29] R. Valero, R. Costa, I. d. P. R. Moreira, D. G. Truhlar, F. Illas. *J. Chem. Phys.* **2008**, *128*, 114103.
- [30] J. P. Perdew. *Phys. Rev. B* **1986**, *33*, 8822.
- [31] T. Kupka. *Magn. Reson. Chem.* **2009**, *47*, 674.
- [32] T. Kupka. *Chem. Phys. Lett.* **2002**, *461*, 33.
- [33] P. F. Provasi, G. A. Aucar, S. P. A. Sauer. *J. Chem. Phys.* **2001**, *115*, 1324.
- [34] V. Barone. *J. Chem. Phys.* **1994**, *101*, 6834.
- [35] V. Barone. in *Recent Advances in Density Functional Methods Part I* (Ed: D. P. Chong). World Scientific Publ. Co.: Singapore, **1996**; p. 287.
- [36] O. B. Lutnæs, T. A. Ruden, T. Helgaker. *Magn. Reson. Chem.* **2004**, *42*, S117.
- [37] U. Benedikt, A. A. Auer, F. Jensen. *J. Chem. Phys.* **2008**, *129*, 064111.
- [38] F. Jensen. *J. Chem. Theory Comput.* **2006**, *2*, 1360.
- [39] L. Hermosilla, P. Calle, J. M. García de la Vega, C. Sieiro. *J. Phys. Chem. A* **2005**, *109*, 1114.
- [40] R. H. Contreras, R. Suardiá, C. Pérez, R. Crespo-Otero, J. San Fabián, J. M. García de la Vega. *J. Chem. Theory Comput.* **2008**, *4*, 1494.
- [41] R. H. Contreras, R. Suardiá, C. Pérez, R. Crespo-Otero, J. San Fabián, J. M. García de la Vega. *Int. J. Quantum Chem.* **2010**, *110*, 532.
- [42] R. Suardiá, R. Crespo-Otero, C. Pérez, J. San Fabián, J. M. García de la Vega. *J. Chem. Phys.* **2011**, *134*, 061101.
- [43] S. Huzinaga. *J. Chem. Phys.* **1965**, *42*, 1293.
- [44] T. W. Keal, D. J. Tozer, T. Helgaker. *Chem. Phys. Lett.* **2004**, *391*, 374.
- [45] M. Pecul, K. Ruud. *Magn. Reson. Chem.* **2004**, *42*, S128.
- [46] T. Ratajczyk, M. Pecul, J. Dadlej, T. Helgaker. *J. Phys. Chem. A* **2004**, *108*, 2758.
- [47] A. B. Yongye, B. L. Foley, R. J. Woods. *J. Phys. Chem. A* **2008**, *112*, 2634.
- [48] T. Kupka. *Magn. Reson. Chem.* **2009**, *47*, 210.
- [49] T. H. Dunning Jr. *J. Chem. Phys.* **1989**, *90*, 1007.
- [50] D. E. Woon, T. H. Dunning Jr. *J. Chem. Phys.* **1995**, *103*, 4572.
- [51] K. A. Peterson, D. E. Woon, T. H. Dunning Jr. *J. Chem. Phys.* **1994**, *100*, 7410.
- [52] A. K. Wilson, T. van Mourik, T. H. Dunning Jr. *J. Mol. Struct. (Theochem)* **1996**, *388*, 339.
- [53] R. H. Contreras, J. E. Peralta, C. G. Giribet, M. C. Ruiz de Azua, J. C. Facelli. *Ann. Repts. NMR Spectrosc.* **2000**, *41*, 55.
- [54] K. Ruud, L. Frediani, R. Cammi, B. Mennucci. *Int. J. Mol. Sci.* **2003**, *4*, 119.
- [55] M. J. Frisch, G. W. Trucks, H. B. Schlegel, G. E. Scuseria, M. A. Robb, J. R. Cheeseman, J. A. Montgomery, T. Vreven Jr, K. N. Kudin, J. C. Burant, J. M. Millam, S. S. Iyengar, J. Tomasi, V. Barone, B. Mennucci, M. Cossi, G. Scalmani, N. Rega, G. A. Petersson, H. Nakatsuji, M. Hada, M. Ehara, K. Toyota, R. Fukuda, J. Hasegawa, M. Ishida, T. Nakajima, Y. Honda, O. Kitao, H. Nakai, M. Klene, X. Li, J. E. Knox, H. P. Hratchian, J. B. Cross, V. Bakken, C. Adamo, J. Jaramillo, R. Gomperts, R. E. Stratmann, O. Yazyev, A. J. Austin, R. Cammi, C. Pomelli, J. W. Ochterski, P. Y. Ayala, K. Morokuma, G. A. Voth, P. Salvador, J. J. Dannenberg, V. G. Zakrzewski, S. Dapprich, A. D. Daniels, M. C. Strain, O. Farkas, D. K. Malick, A. D. Rabuck, K. Raghavachari, J. B. Foresman, J. V. Ortiz, Q. Cui, A. G. Baboul, S. Clifford, C. Pomelli, J. W. Ochterski, B. B. Stefanov, G. Liu, A. Liashenko, P. Piskorz, I. Komaromi, R. L. Martin, D. J. Fox, T. Keith, M. A. Al-Laham, C. Y. Peng, A. Nanayakkara, M. Challacombe, P. M. W. Gill, B. Johnson, W. Chen, M. W. Wong, C. Gonzalez, J. A. Pople. **2004**.
- [56] M. J. Frisch, G. W. Trucks, H. B. Schlegel, G. E. Scuseria, M. A. Robb, J. R. Cheeseman, G. Scalmani, V. Barone, B. Mennucci, G. A. Petersson, H. Nakatsuji, M. Caricato, X. Li, H. P. Hratchian, A. F. Izmaylov, J. Bloino, G. Zheng, J. L. Sonnenberg, M. Hada, M. Ehara, K. Toyota, R. Fukuda, J. Hasegawa, M. Ishida, T. Nakajima, Y. Honda, O. Kitao, H. Nakai, T. Vreven, J. A. Montgomery, J. E. Peralta Jr, F. Ogliaro, M. Bearpark, J. J. Heyd, E. Brothers, K. N. Kudin, V. N. Staroverov, R. Kobayashi, J. Normand, K. Raghavachari, A. Rendell, J. C. Burant, S. S. Iyengar, J. Tomasi, M. Cossi, N. Rega, J. M. Millam, M. Klene, J. E. Knox, J. B. Cross, V. Bakken, C. Adamo, J. Jaramillo, R. Gomperts, R. E. Stratmann, O. Yazyev, A. J. Austin, R. Cammi, C. Pomelli, J. W. Ochterski, R. L. Martin, K. Morokuma, V. G. Zakrzewski, G. A. Voth, P. Salvador, J. J. Dannenberg, S. Dapprich, A. D. Daniels, O. Farkas, J. B. Foresman, J. V. Ortiz, J. Cioslowski, D. J. Fox. **2009**.
- [57] W. T. Raynes, J. Geertsens, J. Oddershede. *Chem. Phys. Lett.* **1992**, *197*, 516.
- [58] R. D. Wigglesworth, W. T. Raynes, S. P. A. Sauer, J. Oddershede. *Mol. Phys.* **1997**, *92*, 77.
- [59] T. A. Ruden, O. B. Lutnæs, T. Helgaker, K. Ruud. *J. Chem. Phys.* **2003**, *118*, 9572.
- [60] R. D. Wigglesworth, W. T. Raynes, S. Kirpekar, J. Oddershede, S. P. A. Sauer. *J. Chem. Phys.* **2000**, *112*, 3735.
- [61] G. E. Maciel, J. W. McIver, N. S. Ostlund, J. A. Pople. *J. Am. Chem. Soc.* **1970**, *92*, 1.

- [62] J. Dantas Vilcachagua, L. C. Ducati, R. Rittner, R. H. Contreras, C. F. Tormena. *J. Phys. Chem. A* **2011**, *115*, 1272.
- [63] R. H. Contreras, T. Llorente, G. I. Pagola, M. G. Bustamante, E. E. Pasqualini, J. I. Melo, C. F. Tormena. *J. Phys. Chem. A* **2009**, *113*, 9874.
- [64] W. Adcock. *J. Phys. Org. Chem.* **2009**, *22*, 1065.
- [65] O. E. Taurian, R. H. Contreras, D. G. Kowalewski, J. E. Pérez, C. F. Tormena. *J. Chem. Theory Comput.* **2007**, *3*, 1284.
- UNCORRECTED PROOF



06 Density functional theory assessment for the determination of one-bond carbon–hydrogen spin–spin coupling constants is examined.
07 Predictions using five functionals and nine basis sets are computed and compared with experimental values. The collection of 68 organic
08 molecular systems with 88 coupling constants includes different types of hybridized carbon atoms. Regression analysis was used as a
09 basic and appropriate methodology for this type of comparative study. B3P86/aug-cc-pVTZ-J yields good results for the studied set.

Author Query Form

Journal: Magnetic Resonance in Chemistry

Article: MRC_4014

Dear Author,

During the copyediting of your paper, the following queries arose. Please respond to these by annotating your proofs with the necessary changes/additions.

- If you intend to annotate your proof electronically, please refer to the E-annotation guidelines.
- If you intend to annotate your proof by means of hard-copy mark-up, please refer to the proof mark-up symbols guidelines. If manually writing corrections on your proof and returning it by fax, do not write too close to the edge of the paper. Please remember that illegible mark-ups may delay publication.

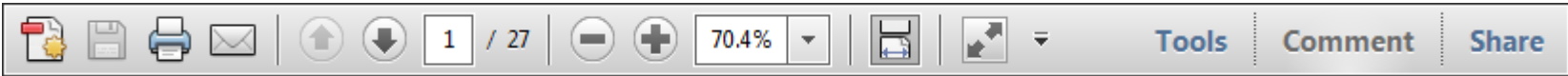
Whether you opt for hard-copy or electronic annotation of your proofs, we recommend that you provide additional clarification of answers to queries by entering your answers on the query sheet, in addition to the text mark-up.

Query No.	Query	Remark
Q1	AUTHOR: 'root-mean-square'. Is this the correct definition for 'rms'? Please change if this is incorrect.	
Q2	AUTHOR: Please check if all tables have been presented correctly.	
Q3	AUTHOR: "acetilene" has been changed to "acetylene". Please check if correct.	
Q4	AUTHOR: "The remaining B3LYP results and those carried out with TZVP...yield large $\sigma^{(rv)}$ values between 7 and 13 Hz." The meaning of this sentence is not clear; please rewrite or confirm that the sentence is correct.	
Q5	AUTHOR: "Thus, in the methane molecule the nuclear densities...all basis sets except the EPRIII and TZVP." This sentence has been reworded for clarity. Please check and confirm it is correct.	
Q6	AUTHOR: Please define FC.	
Q7	AUTHOR: As per Wiley journal instruction, use of above to denote the previous text, table, equation, etc. is avoided. Please check if changes made are appropriate.	
Q8	AUTHOR: "When the carbon involved in the coupling...7.6 Hz (see aforementioned comments about this result)." This sentence has been reworded for clarity. Please check and confirm it is correct.	
Q9	AUTHOR: The four groups of models have been presented in a displayed list. Please check if this is appropriate.	
Q10	AUTHOR: "The remaining models seem...is considered (see Table 8)." This sentence has been reworded for clarity. Please check and confirm it is correct.	
Q11	AUTHOR: Please check acknowledgement section if presented correctly.	
Q12	AUTHOR: Please provide abbreviated journal title for Reference 5.	
Q13	AUTHOR: Please check list of authors for References 55 and 56 if presented correctly.	

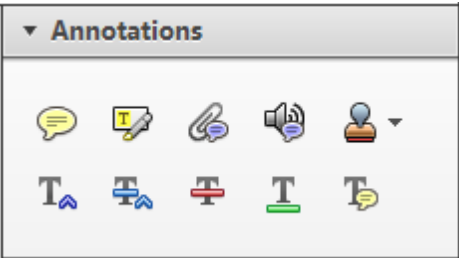
USING e-ANNOTATION TOOLS FOR ELECTRONIC PROOF CORRECTION

Required software to e-Annotate PDFs: Adobe Acrobat Professional or Adobe Reader (version 7.0 or above). (Note that this document uses screenshots from Adobe Reader X)
The latest version of Acrobat Reader can be downloaded for free at: <http://get.adobe.com/uk/reader/>

Once you have Acrobat Reader open on your computer, click on the [Comment](#) tab at the right of the toolbar:



This will open up a panel down the right side of the document. The majority of tools you will use for annotating your proof will be in the [Annotations](#) section, pictured opposite. We've picked out some of these tools below:



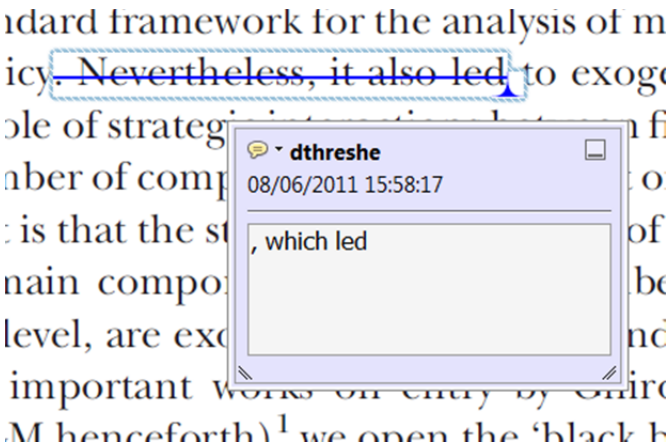
1. [Replace \(Ins\)](#) Tool – for replacing text.



Strikes a line through text and opens up a text box where replacement text can be entered.

How to use it

- Highlight a word or sentence.
- Click on the [Replace \(Ins\)](#) icon in the Annotations section.
- Type the replacement text into the blue box that appears.



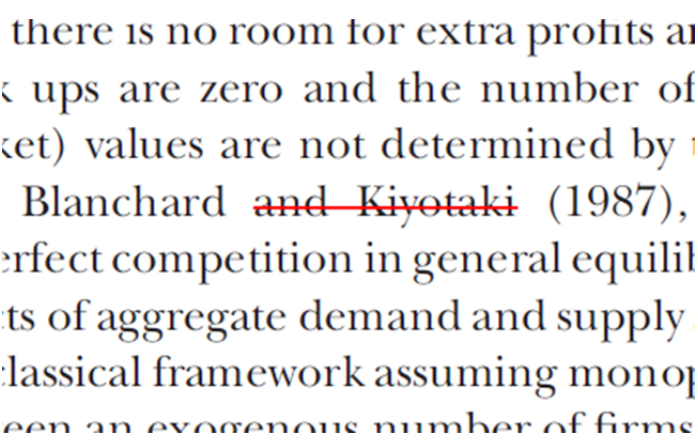
2. [Strikethrough \(Del\)](#) Tool – for deleting text.



Strikes a red line through text that is to be deleted.

How to use it

- Highlight a word or sentence.
- Click on the [Strikethrough \(Del\)](#) icon in the Annotations section.



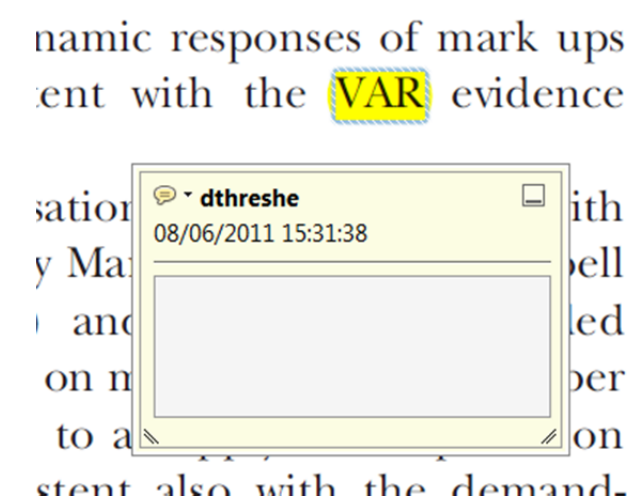
3. [Add note to text](#) Tool – for highlighting a section to be changed to bold or italic.



Highlights text in yellow and opens up a text box where comments can be entered.

How to use it

- Highlight the relevant section of text.
- Click on the [Add note to text](#) icon in the Annotations section.
- Type instruction on what should be changed regarding the text into the yellow box that appears.



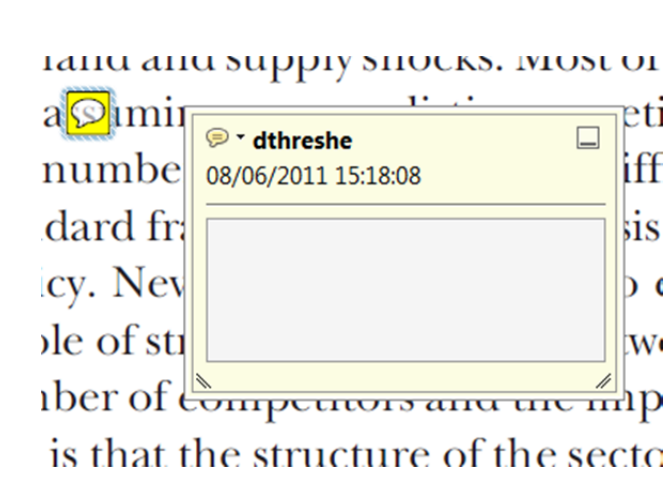
4. [Add sticky note](#) Tool – for making notes at specific points in the text.



Marks a point in the proof where a comment needs to be highlighted.

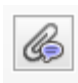
How to use it

- Click on the [Add sticky note](#) icon in the Annotations section.
- Click at the point in the proof where the comment should be inserted.
- Type the comment into the yellow box that appears.



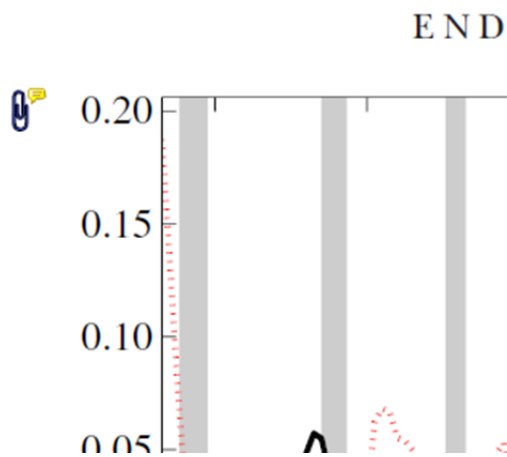
USING e-ANNOTATION TOOLS FOR ELECTRONIC PROOF CORRECTION

5. **Attach File** Tool – for inserting large amounts of text or replacement figures.


 Inserts an icon linking to the attached file in the appropriate place in the text.

How to use it

- Click on the **Attach File** icon in the Annotations section.
- Click on the proof to where you'd like the attached file to be linked.
- Select the file to be attached from your computer or network.
- Select the colour and type of icon that will appear in the proof. Click OK.



6. **Add stamp** Tool – for approving a proof if no corrections are required.

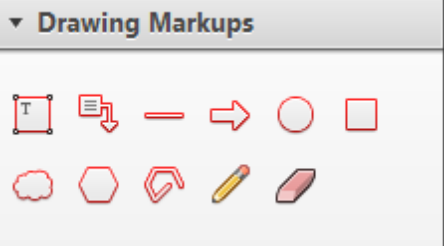
 Inserts a selected stamp onto an appropriate place in the proof.

How to use it

- Click on the **Add stamp** icon in the Annotations section.
- Select the stamp you want to use. (The **Approved** stamp is usually available directly in the menu that appears).
- Click on the proof where you'd like the stamp to appear. (Where a proof is to be approved as it is, this would normally be on the first page).

of the business cycle, starting with the
on perfect competition, constant returns
production. In this environment goods
extra profits and the structure of market
he number of firms in the individual firm
etermined by the model. The New-Key
otaki (1987), has introduced product
general equilibrium models with nominal
ed and supply shocks. Most of this literat

APPROVED

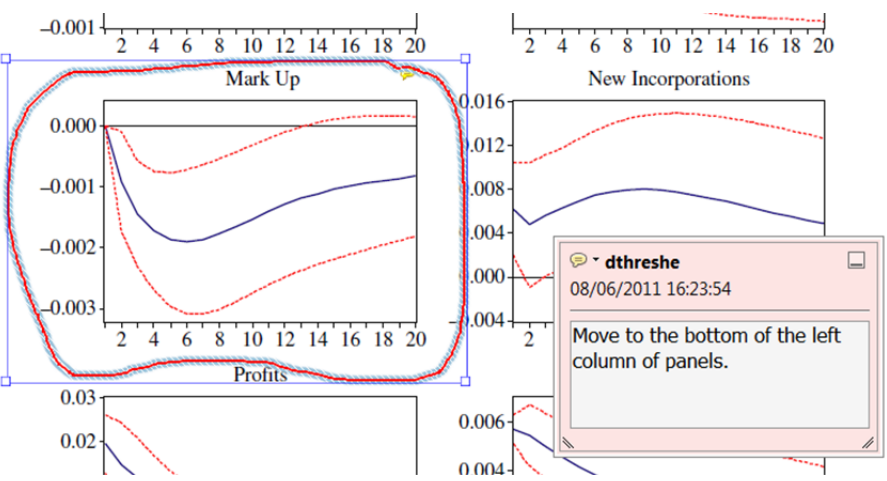


7. **Drawing Markups** Tools – for drawing shapes, lines and freeform annotations on proofs and commenting on these marks.

Allows shapes, lines and freeform annotations to be drawn on proofs and for comment to be made on these marks..

How to use it

- Click on one of the shapes in the **Drawing Markups** section.
- Click on the proof at the relevant point and draw the selected shape with the cursor.
- To add a comment to the drawn shape, move the cursor over the shape until an arrowhead appears.
- Double click on the shape and type any text in the red box that appears.



For further information on how to annotate proofs, click on the **Help** menu to reveal a list of further options:

